Mahnoush Farhang Khaghan Pour

LiDAR mapping connectivity in fractured and deep-weathered bedrock; Implications for fluid migration and storage

Master's thesis in Natural Resources Management

Trondheim, Norway

Autumn 2014

Supervisor: Hans Ola Fredin

Norwegian University of Science and Technology

Faculty of Natural Sciences and technology

Department of Geography

NTNU – Trondheim
Norwegian University of
Science and Technology

Abstract

The precision of high resolution LiDAR data provides a unique opportunity to map geologic features in detail. ArcGIS and 1-m resolution LiDAR data lays down the foundation for detailed geological mapping and understanding. LiDAR data covering the Bømlo area, western Norway, allows generating of a high-resolution digital elevation model (DEM). After the vegetation is filtered away, only bedrock and soils are visible. The 1-m DEM is an excellent asset for image enhancement in GIS to calculate connectivity and surface volumes of the landscape. The study involves GIS image enhancement to extract linear elements (bedrock fractures). Thereafter the extracted bedrock elements are used to calculate connectivity, effective distance and transport pathways for hypothetical hydrocarbons or other fluids. The DEM is also used in GIS to calculate past saprolite volumes which have now been eroded away. Consequently, hypothetical hydrocarbon and fluid reservoir volume is calculated by using the standard porosity (approximately 25%) of saprolite. Finally, the transport capacity of hydrocarbons through saprolite is estimated using the calculated bedrock connectivity and the surface volume. Based on such estimation, this master thesis aims at tackling the reservoir management problem by developing a framework of how to use and evaluate LiDAR data and Geographical Information System (GIS) for future work.

Keywords: Natural resource management, Bømlo, LiDAR data, GIS, hydrocarbon reservoirs, bedrock connectivity, saprolite, surface volume.

To:

Mom, piece of God on the earth

Dad, the spirit of life

My sweet angels Mahgan, Mahroo and Marjan

My supportive and kind brother, Saeed

And the Happiness of life, Tarlan

Acknowledgements:

I want to start these words expressing my sincere gratitude to the people who made it possible for me to come this far with my studies. First of all, my deepest gratitude goes to my supervisor Hans Ola Fredin for all of his guidance, kindness and supports. His comments and advises contributed significantly to this work and his encouragements made it easy for me to accept challenges.

I am also very grateful to Jan Ketil Rød who supported me and helped me to attend this master program. His trust and faith in me gave the confidence to even start my work.

The Natural resource faculty and Geography department should be mention as well. I would like to thank everybody in the department for the nice and warm academic environment.

I cannot thank my family enough for the support which they gave me throughout my studies. Coming this far would not have been possible without their emotional and financial support from miles.

I want to extend my gratitude also to Husoms who became my family miles away from home. Morten, Bente, Peder, Ragnhild and Mikkel Husom supported me in every possible way during the journey of last couple of years in Norway. I will always remember lively moments that I spent with you.

I would like to thanks my real friends who never left me alone and always were there for me. Thank you sweet Yngvild, Peter Wandera, Babak, Tina and Mansoureh. I never forget your helps and kindness. Thanks for caring and sharing your time with me.

Trondheim, Autumn 2014

Mahnoush

Contents

List of figures

List of tables

Abbreviations

Abbreviation	Explanation
A.s.l	Above sea level
DEM	Digital Elevation Model
DSM	Digital Surface Model
DTM	Digital Terrain Model
ESRI	Environment system research institute
GIS	Geographical Information System
Km	Kilo meter
Km^2	Square meter
LAS file	Laser file format
LIDAR	Light Detection And Ranging
m	Meter
m^3	Cubic meter
NGU	Norges Geologisk Undersøkelse
NTNU	Norwegian University of Science and Technology
TIN	Triangular Irregular Network
TWIN	Tropical Weathering In Norway

1   Introduction

"When one tugs at a single thing in nature, he finds it attached to the rest of the world."
-John Muir

Most of the growth in human's life has required exploration of energy sources (Hall, Tharakan et al. 2003). Natural resources support humankind's life. As the population of the world grows at a fast rate, the consumption of energy by humans is increasing each day (Lang 1998).Therefore, it is essential to think about the best way to manage and use resources effectively in a sustainable way. Due to the effects of natural resources on many different aspects of people's lives such as economy, environment and health, the main idea of natural resource management is to manage the costs and expenses of energy production and their sustainability and allow us to make decisions in an informed way (Mallawaarachchi, Walker et al. 1996).

Oil and fossil fuels are some of the most important resources in our daily lives. As the population of the world increases, the demand for these resources is going to increase. This would invariably affect the cost of producing these resources. Increasing the use of petroleum products in daily life and the rising oil prices increase the demand for these resources (Mohn and Osmundsen 2008). Even though both offshore and onshore methods for extracting oil are costly, onshore operations are carried out more easily and cheaper (Gunterberg 2013). Onshore operations such as investigation of reservoirs in bedrock and crystalline basement rocks have produced significant amount of oil and gas in many countries in the world e.g. Venezuela, Brazil, Morocco, Libya, Algeria, Egypt, China, Siberia, Texas, California, Kansas, and Indonesia (Koning 2003). Thus, due to financial interests, it is desired to find methods to explore hydrocarbon reservoirs in crystalline basement rocks on mainland.

In the Norwegian sector of the North Sea, major hydrocarbon resources have been found on the Southern "Utsira High" area at Johan Sverdrup and Edvard Grieg oil fields. These reservoirs are considered unconventional since a part of the reservoir (Edvard Grieg) is directly in weathered crystalline rock, so called saprolite. However, in the other part (Johan Sverdrup), it appears that hydrocarbons have been migrating to the Jurassic sandstone reservoirs of the field through saprolite and basement fractures (forskning.no 2011, geoportalen 2011).

A collaborative field work study by Norges Geologisk Undersøkelse (NGU) and Norwegian Petroleum Directorate aimed at providing a better understanding of deep weathering on Norway mainland (Tropical Weathering In Norway, TWIN project), concluded that the fractured bedrocks are mainly filled with tropical weathered soil (saprolite) (Olesen, Bering et al. 2012). In addition, a new study by (Gunterberg 2013) shows that the age and petrology of Bømlo basement in the west coast Norway is related with the basement of Utsira High. Interestingly, recent 3D-seismic investigations from Utsira High reveal a very similar basement geomorphology to Bømlo.

Bømlo and the West Coast area in Norway consist of many fractures and contain sediments of weathered and eroded soil. Since a large and systematic quantity of the earth's crust is fractured, one of the important phenomena in natural resource and geology studies are fractures (Gudmundsson 2011). Studies on weathered bedrock, which has significant designation in geological survey, and understanding of fracture structures will improve the knowledge about, and provide implications for, offshore hydrocarbon exploration. It is inevitable that offshore reservoir exploration for hydrocarbon reservoirs is very expensive, time consuming and in need of precise data. However, by applying an onshore method it should be possible to obtain new knowledge about fractures pathways. Therefore, according to these studies and information, Bømlo Island becomes an interesting place for onshore hydrocarbon reservoir investigation (Gunterberg 2013).

1.1 Background

During the Mesozoic era, Norway was mostly subjected to a hot/humid to hot/arid climate where deep bedrock weathering and stripping of sediments took place. Therefore, the Mesozoic era created important landscape features in significant parts of Norway, exhibiting deeply etched joint valleys juxtaposed to fresh bedrock inselbergs. Today, the relict Mesozoic landscape has been stripped by Quaternary glaciations and to some extent been draped by glacial sediments. However, the existence of kaolinite and gibbsite in some pockets made geologists believe that this landscape was formed after prolonged weathering of the underlying basement and also belong to a humid and warm climate. In Norway, such deeply weathered surface is called ''Mesozoic surface''. For instance, weathered basement of Melheimfjellet Mountain in Sogn og Fjordane county can demonstrate the sedimentary and erosion process since the Mesozoic era until now (Ramberg 2008).

Relatively little is known about deep weathering of basement in Scandinavia. Pioneering work mainly by Karna Lidmar-Bergström shows that the basement landscape around SW Sweden and Norway is a leftover from tropical deep weathering in (sub-) Mesozoic time, and has been exposed through Neogene exhumation in relatively late geological time (Lidmar-Bergström, Olsson et al. 1999, Lidmar-Bergström, Ollier et al. 2000, Lidmar-Bergström, Näslund et al. 2007). Figure 1 shows schematic illustration of basement weathering process in Scandinavia. In these areas the most direct evidence of ancient deep weathering are pockets of saprolite that still can be found in fracture zones and protected areas (figure 2). Furthermore, onshore-offshore correlations (Riis 1996) showed that this very old basement landscape dips down on the Scandinavian continental shelf and is overlain by Mesozoic and Cenozoic strata, where now, offshore hydrocarbon reservoirs are now found. It is thus clear that (sub-) Mesozoic weathering of crystalline basement bedrock has affected the bedrock morphology in ways pertinent for hydrocarbon resource exploration in offshore Norway (Migoń and Lidmar-Bergström 2001, Migoń and Lidmar-Bergström 2002).
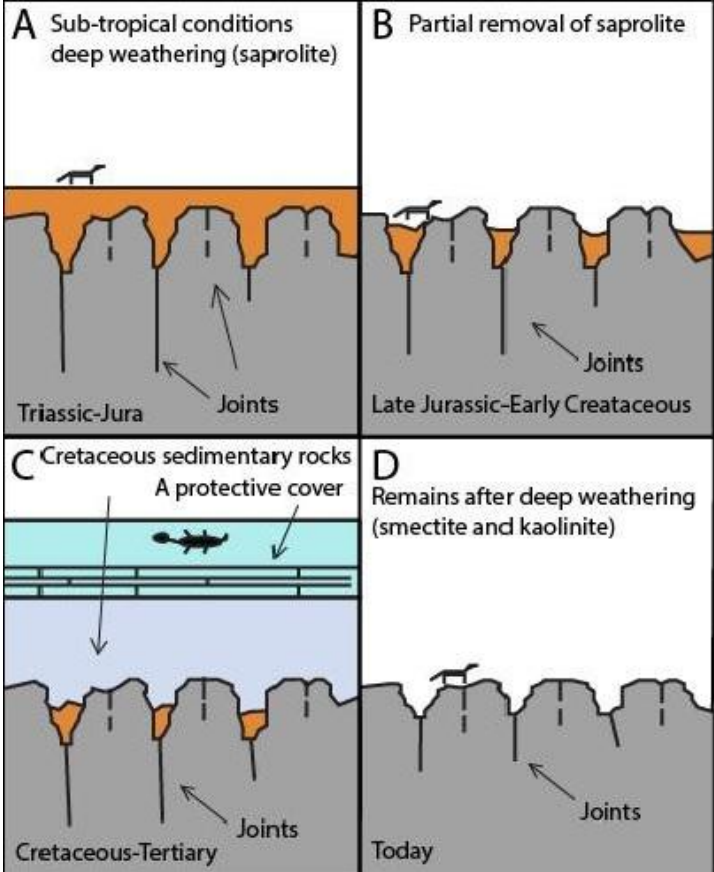
Figure 1: Schematic illustration of basement weathering process in Scandinavia from early Mesozoic time until today, figure from (Gunterberg 2013).

Figure 2: Field work documentation by (Gunterberg 2013), Bømlo, 2013, shows small scale weathered bedrock with typical rounded forms and remnants of saprolite in joint.

During geological time, fractures formed due to stress releases in the Earth's crust and profoundly influenced landscape development, for example by channelizing meteoric water into the bedrock column and thus facilitating deep weathering. Analyzing the Earth crust fractures has increased over the decades due to new technologies such as remote sensing and Geographical Information System (White and Wang 2003). As the exploration and analysis of natural fractures on the earth's crust increased; a relation has been found between the earth's fractures and hydrocarbon reservoirs (Petford and McCaffrey 2003). As hydrocarbons seep through sedimentary fractures, more attention is paid to the nature of bedrock fractures.

Geologically, fracture formations are present everywhere in the world. Occurrence and distribution of fractures have been the interest of oil companies and geologists for decades and have been under consideration of diverse fields of study such as; petroleum reservoir exploitation, water supply exploitation, geotechnical applications, mining and mineralization process (Berkowitz 2002, Gudmundsson 2011) . Many dynamic process of the Earth are largely under the control of rock fractures (Gudmundsson 2011) therefore fracture analysis possesses positive influence for exploration and development in many geological natural resources. Determination of fractures' effects on natural reservoirs gives a possibility to be detailed and correct in the reservoir finding process. Indeed finding fractures is not enough but it is one of the most important and basic steps for evaluating fractured reservoirs and analyzing them helps in understanding the geological processes behind a fluid reservoir (Nelson 2001). Thus, they count as a clue for water, oil and gas reservoirs exploration (Petford and McCaffrey 2003).

1.2 Motivation

The landscape, both at Utsira High and Bømlo consists of a joint-valley landscape where faults cross each other and create depressions with intermittent bedrock knolls (Gunterberg 2013). In the depressions, weathering soil can be found which shows that the fractured landscape experienced deep chemical weathering prior to Mesozoic burial and later exhumation (Olesen, Bering et al. 2012). Some of the world's hydrocarbon reservoirs come from fractured reservoirs (Nelson 2001) and it is observed that crystalline basement reservoirs can be very prolific specifically where they are highly fractured (Petford and McCaffrey 2003). Assuming that Bømlo is a good analog to Southern Utsira High, many interesting questions can be answered more easily in an onshore manner compared with the costly seismic and drilling operations in off-shores methods.

There have been studies conducted on weathered basement rocks in Norway as well as Bømlo island, e.g. (Gunterberg 2013) has performed a study on the remnants of weathered rocks in Bømlo in order to find out the occurrence of oil in the crystalline bedrock. In such a study, mostly geological issues like age; petrology and weathering of basement rocks were under consideration, hence it was involved sampling and observing the weathered materials. Also the TWIN project stated that deeply weathered bedrock is a widespread phenomenon in parts of mainland and offshore Norway. In the TWIN project, numerous occurrences of deeply weathered bedrock have been studied and the study found out that remnants of weathered basement rocks in Norway have considerable potential for hydrocarbon and groundwater reservoirs (Olesen, Bering et al. 2012). The interests of most of the studies have been on the age and petrology of weathered bedrock. Besides, the related studies have been in the field of geology and no one has mapped the fractured bedrock structures in small scale.

In comparison to oil production from conventional reservoirs, exploring oil from fractured reservoirs incurs different challenges (Haugen 2010), and therefore one of the early steps for evaluating and planning of reservoirs is understanding the effect of natural fractures as early as possible (Nelson 2001). For evaluating the fractures' connectivity, one of the necessities is studying the outcrop of exposed fractures and also density, length, orientation, and spatial distribution (Loosveld and Franssen 1992) .Particularly, well exposed rocks can be used to infer analog information for reservoirs (Odling 1994).

Moreover, fluid migration in deeply buried rocks has been an interesting subject for petroleum engineers and hydrologists (Brace 1980). At the same time, fractures effect fluid migration on subsurface either by enhancing or inhibiting flow (Snow 1969, Odling 1992). As a result, fractures can control and influence geological behaviors of fluid storage (Roy, Perfect et al. 2010). Considering the fluid flow behavior in strata, has noteworthy character for managing hydrocarbon reservoirs and aquifers (Willis and White 2000).

Overall, reservoir structure can be studied in detail to obtain information about geometric features, structure, connectivity, permeability and porosity of the area (Gluyas and Swarbrick 2009). Consequently, understanding the characteristics of basement bedrock and saprolite is a key conduit for onshore investigations e.g. hydrocarbon, groundwater.

Electronic instruments and monitoring software have a significant function in different fields of natural science. Thus, mapping the geological outcrop of the earth's surface, especially using the remote sensing method, is a common element and one of the primary methods for exploring petroleum or water resources (Vincent 1997, Rutter 2012). Accordingly, accurate geological and lineament mapping is a critical task for diverse structural analysis (Chaabouni, Bouaziz et al. 2012) and has been recognized as an alternative solution for petroleum exploration and a considerable subject in problem solving in different fields of engineering e.g. hydrological research and geological survey (Argialas and Mavrantza 2004).

Nowadays, there are many available precise methods to survey the surface of the planet. The derived data from these methods plays a significant role in the topography of the specific geography. Thus, this type of data can be the basic input data in Geographical Information System (Schröder and Rossbach 1994). Geographical Information System (GIS) is a suitable application for natural resource managers and also for other operators in diverse fields of science. GIS tools offer lots of possibilities for modeling, storing, managing and evaluating data. Outputs from GIS could be varied and flexible. Creating models, maps and being up to date are prominent advantages of GIS (DeMers 2009).

Today, Digital Terrain Models are mostly compromises between preferred high resolution and (reasonable) cost (Schröder and Rossbach 1994). Furthermore, (Zhou and Chen 2011) suggested that if a terrain parameter of a land surface is identified, calculated and modeled correctly, the other relevant terrain parameters can be extracted truthfully. Mapping in GIS is the final result of a sequence of data processing steps. They are assumed to be the main

supporting tools for decision making with the ability of storage and communication (Longley 2011).

The purpose of this study is to identify bedrocks fractures in the (almost) center of Bømlo Island, as a test to assess the relationship between fractures connectivity and saprolite volume which may impact hydraulic parameters such as hydrocarbon or water reservoirs. Detecting fracture connectivity and estimating the saprolite volume provides more details and data by correlating the available onshore and offshore data in Bømlo. This study has its focus on onshore fracture analysis by GIS as an alternative to solve a related offshore petroleum problem. Correlating the vast amount of existing seismic and well data with the major weathering surfaces occurring on main land could overcome the lack of onshore data (Riis 1996).

Attempting detailed studies of offshore hydrocarbon reservoirs is very expensive and conclusive results are difficult to obtain due to lack of data. By using an onshore analog, considerable new knowledge about pathways and transport behavior of hydrocarbons through fractured and weathered basement bedrock can be obtained. This knowledge is sought out throughout the oil industry of Norway and may play a role in current and future exploration and appraisals of offshore oil fields of Norway and elsewhere.

1.3   Objective

It is inevitable that offshore reservoir exploration for hydrocarbon reservoirs is very expensive, time consuming and in need of precise data (Hesthammer and Boulaenko 2005). Significant knowledge about hydrocarbon reservoirs can be obtained through onshore studies by studying the pathway of the earth's fractures and their influence on hydrocarbon migration. However, by applying an onshore method it should be possible to obtain new knowledge about the pathways of fractures. The knowledge that will be obtained through this study can play an important role in current and future explorations, and appraisals of offshore oil fields in Norway and other places.

General

The following research aims at developing a hypothetical method to extract bedrock fractures connectivity and calculate the eroded saprolite volumes, from LIDAR data and high resolution DEM.

Specifics

To carry out the main objective, the following specific tasks have been applied:

- Image enhancement for lineament extraction

- Extracting pathways manually and automatically

- Measuring the eroded away saprolite in fractures at specific hypothetical thickness intervals

- Estimating the amount of potential reservoir a typical weathering landscape has by using porosity of the eroded saprolite

Research questions

For study hypothesis, the following questions, pertaining to bedrock morphology on Bømlo, will be pursued;

1. What are the connectivity and pathways in the study area?
2. How large are the volumes of saprolite in the study area?
3. How large are the oil reservoir volumes in saprolite in this type of landscape?

1.4 Definitions of used terms

1.4.1 Geographical Information system (GIS)

Every minute in every place of this big world something is happening at a point. In geography, points and locations are the most important and fundamental issue. Location may have different definitions in diverse fields of engineering and science. The common and most widely known meaning refers to a special point or position in physical space. Human beings perform a wide range of activities on the Earth like constructing, creating, digging, destroying and so on in addition to natural activities (Longley 2005). Tracking and knowing the location of these activities can be significantly important and helpful to have information about the location (Longley 2011).

Explaining and defining GIS is not an easy task since this technique is so vast and includes a wide range of applications. In some, cases people look at GIS as a branch of IT science and others know this technology as a computer-based assistant for producing maps (Yeung and Lo 2002). Many definitions have been proposed for GIS. In order to provide a definition of GIS for understanding the general idea and for the benefit of the readers, we have decided to respectively use the definition of GIS from known authors and organization;

"A computer system that can store virtually any information found on a paper map. But it can be much more helpful than a traditional map…" (Korte 2001).

"This system is as a chain of functions start from planning the observation and collection data, to store and analysis of the data, to the use of the derived information in some decision making process. GIS refers to an information system that is designed to work with data referenced to spatial or geographic coordinates" (Ramachandran 1998).

According to the United States Geological Survey (USGS) ''A GIS is a computer system capable of capturing, storing, analyzing, and displaying geographically referenced information; that is, data identified according to location. Practitioners also define a GIS as including the procedures, operating personnel, and spatial data that go into the system'' (USGS 2007).

Lillesand, Kiefer et al. (2004), described Geographic information System is as a computer-based system which can virtually deal with different types of feature information. Such a system is capable of managing both location data and attribute data of features.

1.4.2   Light Detection And Ranging (LiDAR)

Light Detection And Ranging (LiDAR) is an active optical remote sensing method that uses laser light. In this case, the active optical sensor uses light in form of pulsed laser while flying above a specific surface (Schmid, Waters et al. 2008). The reflections of transmitted laser beams generate precise three dimensional coordinates of the investigated desired surface. The result of such process is a dense and detailed group of points, called "point cloud''(Kreylos, Bawden et al. 2008). Point cloud datasets are large collection of 3D elevation points that can be analyzed and visualized in ArcGIS (ESRI 2013). Usually, the major hardware LiDAR system consist of a laser scanner, a GPS (Global Positioning System), an INS (Inertial Navigation System) including IMU (Inertial Measurement Unit) and a collection vehicle to fly over the surface such as aircraft (Song, Han et al. 2002). Figure 3 shows the LiDAR system hardware.

The main advantage of the LiDAR technique is to present a direct method for collecting 3D data collection (Shan and Toth 2008). Therefore, this method has frequently been applied to map the Earth's surface since the derived data from this method provides the possibility to produce high resolution digital elevation models (DEMs) or Digital Terrain Models (DTMs) (Ventura and Vilardo 2008). Moreover, this method is able to generate geo-referenced DEM (Zhiqing, Huirong et al. 2006).

The possibility of gaining information about topography of desired land makes this technique a suitable method for studies in natural resource monitoring, geology, hydrology and geotechnical engineering. For these reasons, during the past decade, LiDAR has extensively become famous as a perfect and speedy 3D technique for Earth surface survey (Zhiqing, Huirong et al. 2006) such as in geology, geomorphology and hydrological modeling (Glenn, Streutker et al. 2006, Cavalli, Tarolli et al. 2008, Ventura and Vilardo 2008).

Before LiDAR became the preferred method to measure topography, other traditional methods like photogrammetry and field surveys were the tools for producing DTMs. LiDAR technology has made revolutionary progress in producing high-resolution DEM (Neri, Mazzarini et al. 2008) by flying over a large surface and consequently save quite a lot of time, cost and manpower (Zhiqing, Huirong et al. 2006). Although the traditional methods can provide high quality DTMs, they take more time and effort compared to the LiDAR method. In addition, while steep slopes or high biomass exist on a surface, traditional DTM generation methods are difficult to implement (Tinkham, Huang et al. 2011).
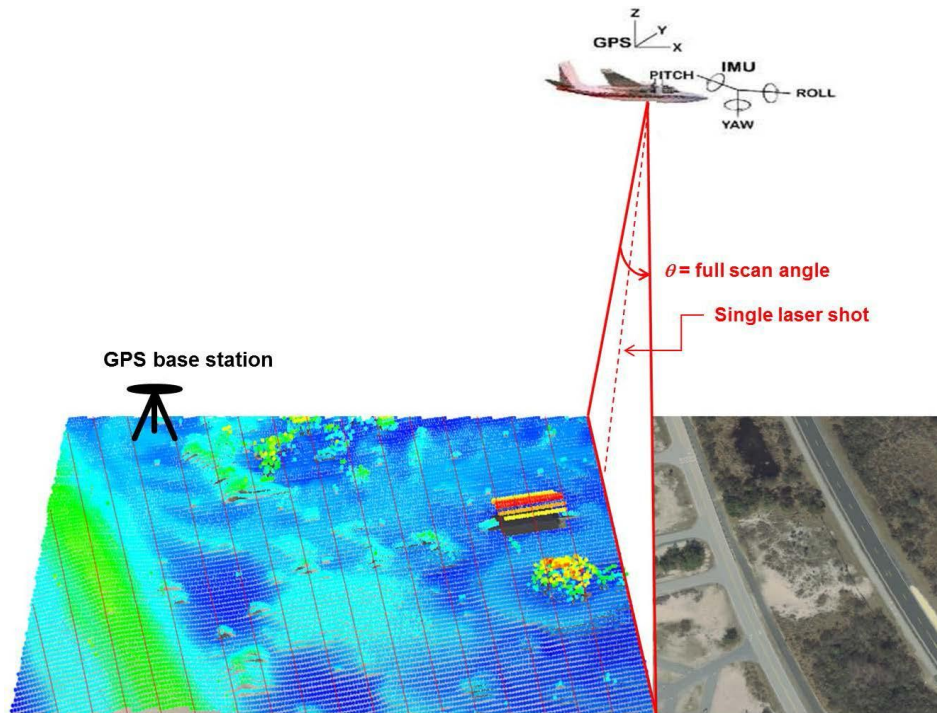
Figure 3: LiDAR system components , figure from (Schmid, Waters et al. 2008).

1.4.3 Digital Terrain Models

Terrain information is fundamental for use in many disciplines and fields of study such as geography, earth and environmental sciences and resource (Yeung and Lo 2002). Surfaces of all kinds are very common in GIS, but because of their three dimensional nature, they force additional requirements on the computer programmer who wants to represent them (DeMers 2009). It is suggested that different terms for terrain models refer to different products and concepts (Li, Zhu et al. 2010).Therefore, for representing the terrain surfaces, it is essential to explain their concept and their differences. Due to these slight differences of terrain models, it is considered to explain them separately as the following;

1.4.4 Digital Surface Model

Digital Surface Model (DSM) demonstrates the earth's surface including all objects on it. Such terrain model contains the information about the elevations of natural terrain features including terrain features, buildings, vegetation and other manmade features (figure 4, a). Therefore, it is defined as a terrain model which provides a topographic model of the earth's surface that includes very realistic information (Schmid, Waters et al. 2008)

1.4.5 Digital Terrain Model

The Digital Terrain Model (DTM) is used to represent the bare ground surface of the earth apart from any man-made features. Digital Terrain Model is produced while all man-made and vegetation features digitally removed from a Digital Surface Model, and thus they provide only a topographic model of the bare earth (figure 4, b). The concept of terrain model have been defined as: " the digital terrain model (DTM) is simply a statistical representation of the continuous surface of the ground by a large number of selected points with known X, Y ,Z coordinates in an arbitrary coordinate field" (Li, Zhu et al. 2010).

Simply, DTM is used to demonstrate land surface point elevation. It is assumed that DTMs are topographic models of the bare earth that can be operated and controlled by softwares. These models are the basis for many applications. In GIS , DTMs used as input processing that can help construct surface models, investigate and demonstrate phenomena connected to topography (Weibel and Heller 1993). Since 1950's, DTMs have been used in geosciences applications and also in Earth and engineering science (Miller and Laflamme 1958). In most cases, DTM represents the earth's surface in 3 dimensions and for that reason the DTM data sets are enormously practical for the creation of 3D renderings of any location in the area described. Thus, the rendered 3D models can be use in many applications such as geography, geodesy, geology and engineering (Koch and Heipke 2006).

Recently, Digital Terrain Models' development has been recommended by both researchers and resource managers involved in evaluating land surface elevations (Tinkham, Huang et al. 2011). It is confirmed that LiDAR DTM is more competent and precise as compared to traditional methods (Hodgson, Jensen et al. 2003). The most popular and potential applications of a reliable application of DTM can be named as: extraction of terrain parameters, Visualization of the terrain, Terrain analysis in morphology and cartography, rectification of airborne or satellite images, channel network, and hydrologic modeling (DeMers 2008, Liu and Zhang 2008, Bater and Coops 2009, Spaete, Glenn et al. 2011).

1.4.6 Digital Elevation Model

A digital elevation model (DEM) is a most common raster surface model in three dimensions (3-D), which represents the terrain's surface. This model is subset of DTM model. In other words, DEM can be defined as any numeric or digital representation of surface elevation. This

means that heights are available at each point in the area of interest (O'Callaghan and Mark 1984, Hodgson, Jensen et al. 2003, DeMers 2009).The word elevation in DEM refers to measurement of height above datum (Yeung and Lo 2002). Therefore such model is the most common cell-based digital elevation model in computer-based science for representing continuous surfaces like the earth's surface (ESRI 2011).

Digital elevation models may be created by different techniques such as measurements, photogrammetric method, and LIDAR laser measurements. DEMs derived from airborne LIDAR data have considerably been increased due to high resolution and quality. Therefore, in many hydrologic, geologic and earth science applications apply digital elevation models (DEMs) to gain absolute surface elevation and terrain form information (Hodgson, Jensen et al. 2003).
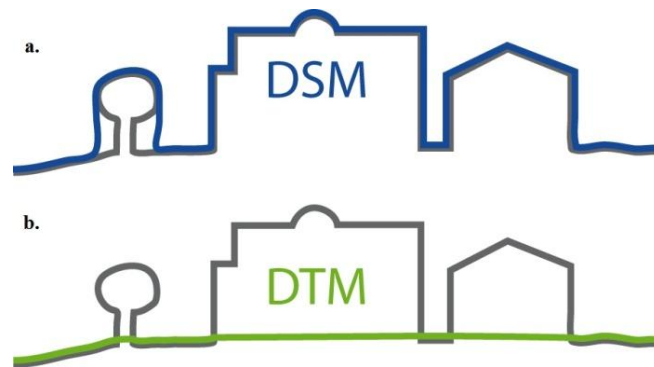
Figure 4: Schematic illustration of digital terrain models, a.) Digital Surface Model presents Earth's surface including all objects, b.) Digital Terrain Model demonstrates the bare Earth surface, figure from (EIJ 2014).

1.4.7   Bed rock

Bedrock is the native and solid rock beneath the surface of the terrestrial planet or material such as soil and sediments. Bedrock can extend thousands of meters below the surface of the Earth, to the crust/mantle bounder and are present everywhere, whether exposed at the surface in outcrops or buried beneath shallow deposits or water. The bedrock has formed over vast periods of geologic time ranging and often classified into three types of lithology based on origin : sedimentary, igneous and metamorphic. Bedrock makes a large proportion of soil parent material and therefore, the mineral composition and grain size of the bedrock strongly influence the type of soil formed. Figure 5 shows the common soil profile where, the deepest part of profile (horizon D) belongs to bedrock layer (Survey 2013, Geographic 2014).

Figure 5: Soil profile horizons, horizon D demonstrates bedrock layer, horizon C presents weathered bedrock (saprolite), figure from (metropolis 2013)

1.4.8 Saprolite

Rocks can be weathered by water and air up to hundred meters in depth and form saprolite. The term of saprolite coined by Becker in 1895 and derived from Greek word (sapros) stand for "rotten" (Taylor and Eggleton 2001). Saprolite can be defined as the following:

"The highly weathered rock is termed as saprolite" (Graham, Rossi et al. 2010).

"A soft, fully decomposed rock that is formed in situ in tropical areas by the chemical weathering of igneous or metamorphic rocks'' (MichaelAllaby).

''Bedrock may weather below its upper surface, forming saprolite'' (Kessarkar and Srinivas).

As a result, saprolite is a name which is given to weathered rock which has retained its original rock volume and structures (Ollier 1988). Saprolitic soils have a tendency to maintain the structure of the parent rock, such that relict faulting and joint patterns are also observed in the soils. This feature can be noteworthy in hydrogeologic evaluations (Poehls and Smith). To distinguish or test the exposed soil to find out whether it is Saprolite or not, saprolite is usually be crumbled by hand and when it gets wet, it forms a plastic (Graham, Rossi et al. 2010). Figure (5) presents the saprolite layer, horizon C.

14

1.4.9   Crystalline rock (Basement rock)

The term 'basement rock' and 'crystalline rock' generate a variety of definitions (Koning 2003). Generally, the standard definition of crystalline rock by most geologists is considered as the rock which is overlain by a sedimentary sequence (Petford and McCaffrey 2003).

1.4.10 Fractures and lineaments

Generally linear features in geology are divided into two categories; Lineaments and Fractures. Therefore, the difference of these two features is about their length. Lineaments are defined as those linear features which their length is greater than one mile while fractures are defined as linear features with total or less than one mile length (Gudmundsson 2011).

1.4.11 Rock Fracture

Fractures are the most common structures on the Earth's surface outcrop. Scientifically rock fracture is any kind of mechanical break to rock body which makes the rock apart into more pieces (Gudmundsson 2011).

1.4.12 Porosity and porous rock

Porous is the capacity of a medium (e.g. rock) to hold fluid. Porosity consider as void spaces in the rock (Gluyas and Swarbrick 2009) or the ratio of pore volume space to its total volume of a medium (Bear 2013)(figure 6). Porosity reported either in percentage from 0 to 100 or as division between 0 to1. Porosity of reservoirs is different hence most of them contain > 0% to < 40 % (Gluyas and Swarbrick 2009).
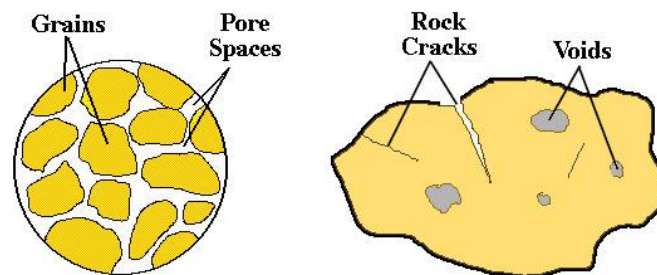
Figure 6: Represents the porosity of a rock, figure from (cmex 2014)

1.5 Study area

Bømlo /ˈbʌmˌloʊ/ is an island located in south west of Norway in southern part of the Hordaland county. This area roughly covers the regions between N 59˚ and E 5˚. For this master thesis, the study area is 1km^2 area almost in the center of the Island (figure 7). This area has recently been the subject of studies regarding to hydrocarbon reservoir that provides new geology information about similarities between Bømlo and Utsira High (Gunterberg 2013).
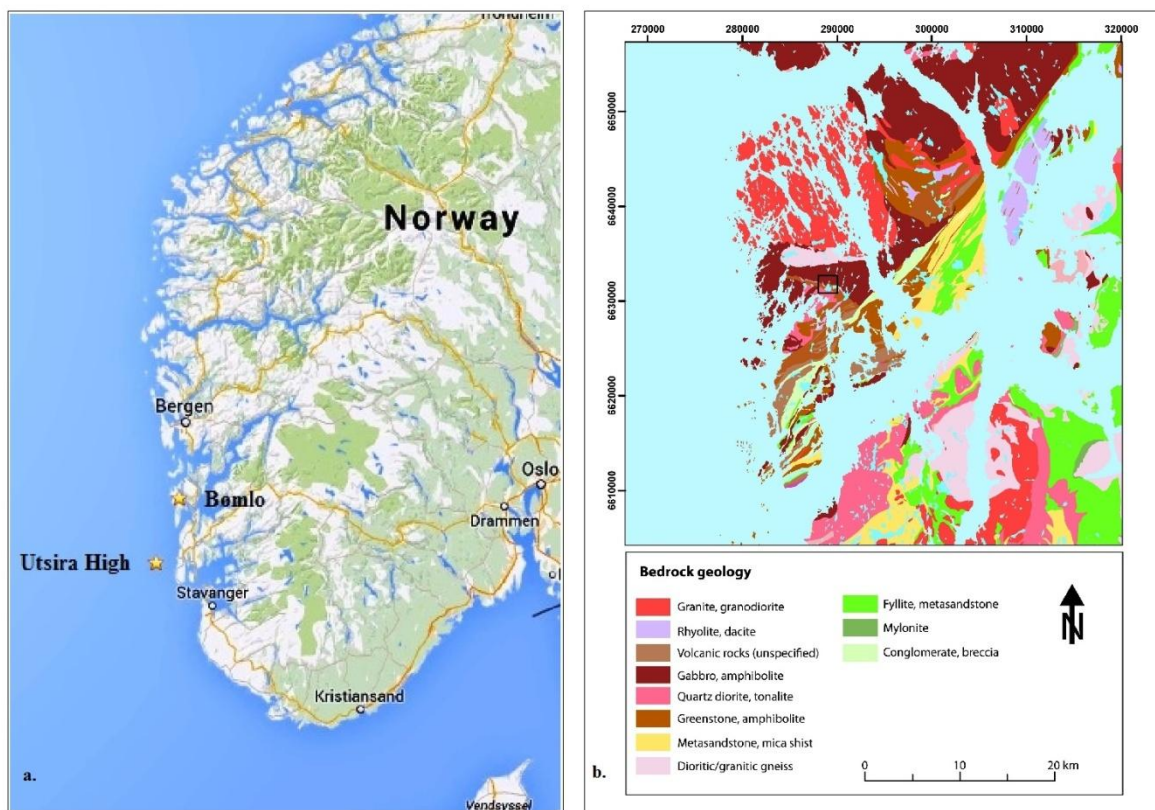
Figure 7: a.)The location of Utsira High and Bømlo in Norway, figure modified from Google map, b.) Geological map of Bømlo modified from www.ngu.no. The small black box in figure 5.a) refers to 1x1 km study area in Bømlo.

2   Methodology

This chapter explores the methods used to generate and analyze data to determine connectivity and pathways, determine how large the volume of Saprolite is and finally determine how large is the oil reservoir volume in Saprolite of the landscape of the study area , Bømlo Island. This study is limited to extraction of bedrock fractures from DEM using ArcGIS. ArcGIS software offers a variety of tools for this purpose, out of which this study utilizes DEM filtering and Hillshading. For an overview of the whole workflow in the study see figure 9.

2.1   Data types

Like most elevation data, LiDAR data can be stored in a different of formats. The raw data are delivered as points or known as "point clouds" (literally clouds of point where each point has x, y and z coordinates). Such point data defined as three dimension point clouds with dense values and other spatial attributes such as GPS time indications, elevations and any other object that has been recorded by laser beam during the survey of a given area. LiDAR data are commonly stored in the LAS format (Liu, Peterson et al. 2005, ESRI 2013). For this research, LiDAR point clouds were obtained from Kartverket, The Norwegian mapping Authority, (www.kartverket.no). From 2007 to date, the Norwegian Mapping Authority has obtained LiDAR data for many parts of Norway, which the Norwegian University of Science and Technology (NTNU) has full access to this raw laser data.

2.2   LiDAR data conversion to Digital Elevation Model

Using ArcCatalog application a LAS dataset was created in a folder. Then the X, Y coordinate system was set to WGS-1984-UTM-Zone-32N. These coordinate and projection systems were chosen because the study area is located in UTM zone 32N. The elevation values were set for defining the geoids height to NN54. The"z" values were important in a sense that they helped to generate the 3D based on elevation values. These operations were followed by adding LAS files into the created LAS dataset. Statistics were used to estimate the spacing for each point cloud and determine classification codes for land cover. The resulting data products used for DEM generation are irregularly distributed ground 3D points (point cloud), with an average spacing of about 1 point per square meter. To enable the creation of a bare-earth DEM, it is necessary to separate ground returns pulse from non-ground other pulses such as buildings, vegetation and tree canopy. Therefore, post-processing of point cloud was performed filtering out all pulses expect "last return" to create a DEM devoid of land cover. It should be noted

that all processes were done in the LAS dataset properties dialog box in ArcMap 10.1. Hence the ground points were incorporated to generate a raster DEM of the area (figure 8). The accuracy of the used LIDAR data is estimated to nearest decimeter (dm) vertically and nearest 5 cm horizontally. Finally, for this study, all the DEMs were interpolated with 1 m resolution, which is considered as a high resolution DEM. See figure 9 for workflow steps.

2.3   Clipping of the study area

The desired area of interest is about one kilometer to one kilometer surface on south west of Norway in Bømlo Island. The place is just a random place on Bømlo with a representative set of fractures and little water areas. In ArcGIS ''Clip'' function is a GIS operation that takes out features from a raster dataset within a defined border by the extend of a feature class. Either in raster or vector dataset, clip tool creates new feature class of desired area base on the chosen pattern shape. The result is output feature class with the same attributes of the input feature class (ESRI 2013). This tool has been used to cut out one kilometer by one kilometer of Bømlo Island; therefore the output of this process is the study area.
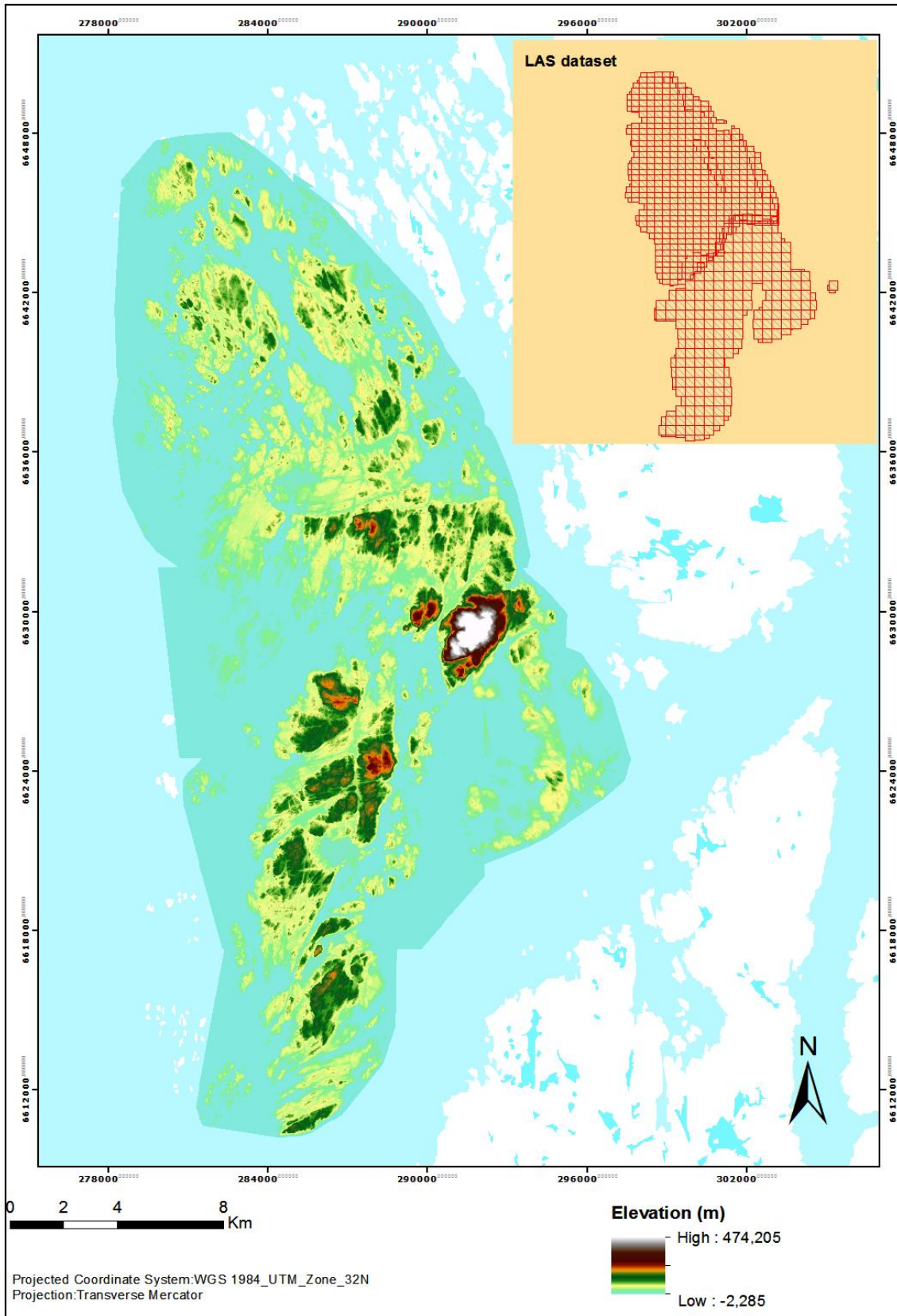
Figure 8: Bømlo Digital Elevation Model derived from LiDAR data. The inset map is Bømlo LAS dataset.

Workflow diagram:
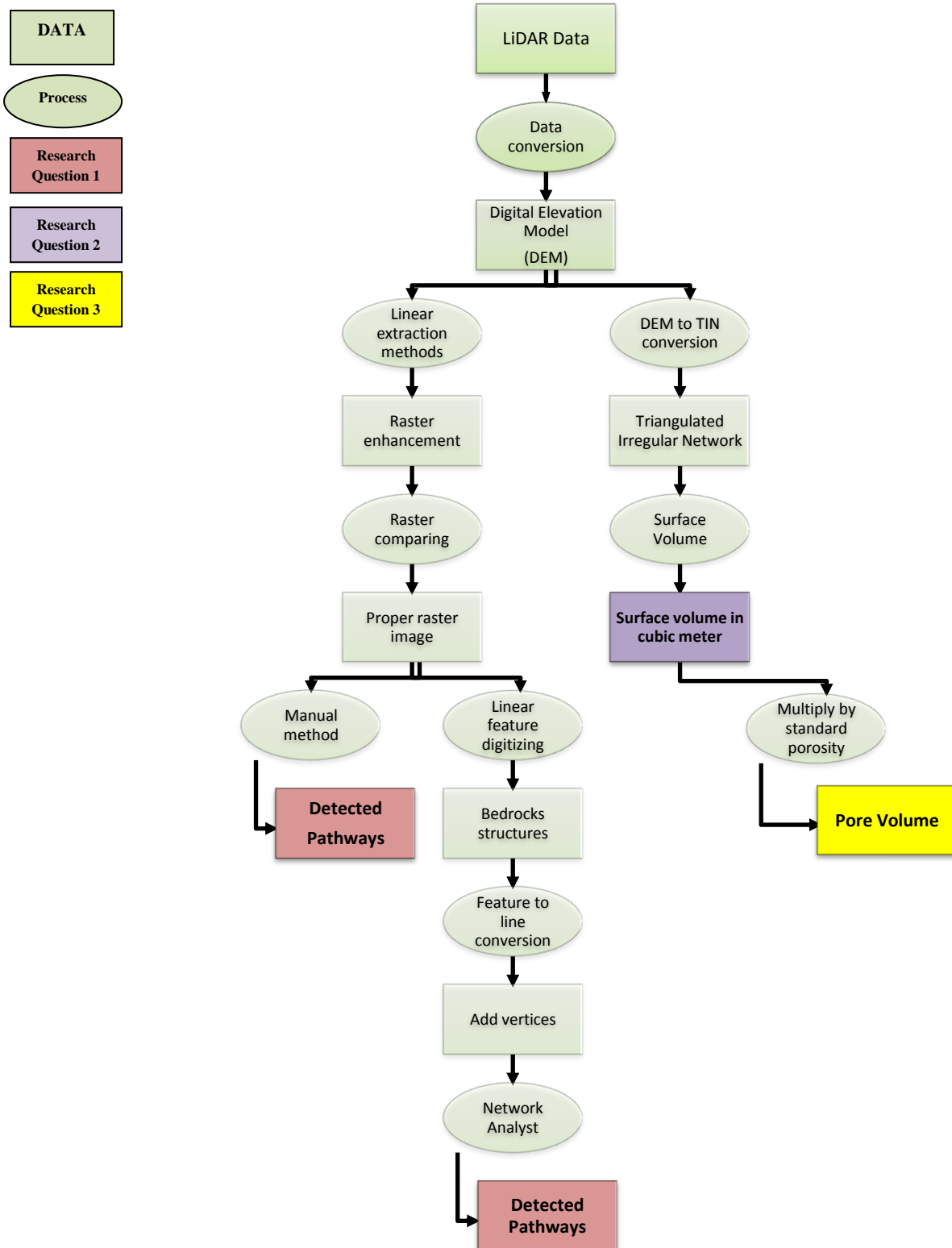
Figure 9: Workflow diagram presents the methods steps.

2.4   Linear feature extraction

There are many linear enhancement techniques available for remote sensing data which is based on highlighting the distinction between the features in the image and it produces better visual quality of the image (Chen, Latifi et al. 1999). Automatic linear feature detection is not available in Arc GIS 10.1. Thus detection of linear features could be done manually in the Arc GIS environment (Geomorphology 2013) (figure 9). For this study two methods are considered for linear feature extraction;

   i.   Filtering of the DEM
  ii.   Hillshading of the DEM

2.4.1   Filtering method

A filter in GIS is commonly a moving window, kernel, with an algorithm being applied to the raster within this moving window (figure10). This can for example reduce or enhance features, depending on feature wavelength in order to improve features or eliminate some data (DeMers 2009). This method is often used in image processing (Lillesand, Kiefer et al. 2004). In GIS can use in raster data processing in to reclassify cell grids based on different filter values (DeMers 2009). In Filtering the weight of each central point evaluates by calculating how cell can be estimated by its neighbor's cells (Zhou and Chen 2011). Filter window could be of various size, and moves systematically across the entire raster coverage in serpentine mode until all cells has been processed (DeMers 2009). There are various types of functions for filters in digital image processing and remote sensing. These includes edge enhancement, noise removal, isolating edge and linear features (DeMers 2009, Ahmed 2011). Overall, filters try to classify a scale component in an image (Walford 2002) and therefore depending on the type of filter, output could be different.
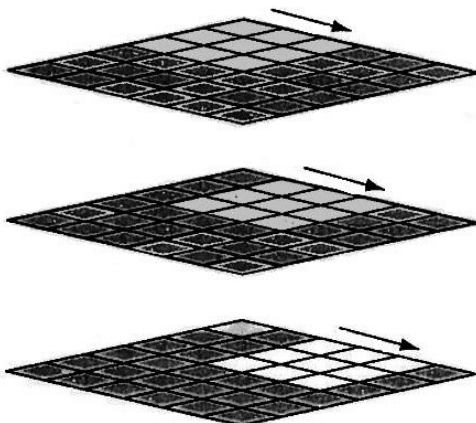
Figure 10: Filter moving window is scanning the raster coverage, from left to right. Figure modified from (DeMers 2009)

2.4.1.1 Convolution filters

The image analysis tool provides many enhancement functions for the image processing. The most commonly used filters for edge detection in GIS are: Laplacian and Sobel filters. Under the processing function of image analysis tool, the add function of tool was used to open the raster function editor so functions can be added, edited, or removed to the selected layer, and create a temporary layer. Within the raster function editor, the DEM was right clicked to access insert option from where convolution function was found. The convolution function performs filtering and the pixel values in a raster which can be used for sharpening an image, blurring an image, detecting edges with an image or other kernel-based enhancements. The LiDAR derived DEM was used as the input raster for convolution within raster function properties. Different types of windows were tested as shown in figure 11(a-f); Sharpening 3x3 and 5x5, Laplacian 3x3 and 5x5, Sobel vertical and Sobel horizontal were used.

Figure 11: Convolution filter matrices. a) sharpening 3x3, b) Sharpening 5x5, c) Laplacian 3x3, d) Laplacian 5x5, e) Sobel horizontal 3x3, f) Sobel vertical 3x3.

2.4.2 Hillshading method

One of the methods for visualizing a DEM is the hillshade technique. This technique is often used for two-dimensional terrain visualization (Yeung and Lo 2002). A hill-shade is an imaginary surface illumination by calculating illumination values for each raster cell based on synthetic solar azimuth and altitude (Witzke, Anderson et al. 2010). Such a technique is applied and used to present surfaces in grayscale (ESRI 2013) and assist to bring out small variations in elevation data (Schmid, Waters et al. 2008). Hill-shading is broadly used as a technique for terrain visualization (Lukas and Weibel 1995) which can calculate the local illumination and determine whether the cell will be in shadow or not. The hillshade function in GIS uses *azimuth* and *altitude* properties to signify the location of light source for example the Sun.

Azimuth is an angular measurement in a spherical coordinate system that is a clock wise angle from a point of an origin to a point of interest (USGS). ESRI define the Azimuth as "the angular direction of the sun, measured from north in clockwise degrees from 0 to 360" (ESRI 2014) (figure 12). This function is use for illuminating a surface from a specific direction (angle). Table 1 presents 16 different north-based azimuth angles.
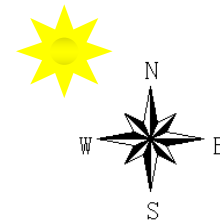
Figure 12: Schematic illustration of the default azimuth angle,315, northwest.

Table 1: Clockwise North-based azimuth angles for illuminating a surface, the highlighted boxes are the used azimuth for hillshade models

Azimuth from North			
North	0˚ or 360˚	South	180˚
North-Northeast	22.5˚	South-southwest	202.5˚
Northeast	45˚	Southwest	225˚
East-Northeast	67.5˚	West-Southwest	247.5˚
East	90˚	West	270˚
East-Southeast	112.5˚	West-Northwest	292.5˚
Southeast	135˚	Northwest	315˚
South-Southeast	157.5˚	North-Northwest	337.5˚

Altitude is the slope or angle of the illumination source (e.g. sun) above the horizon. The units are in degrees; from 0 (on the horizon) to 90 (overhead) (figure 13). Usually altitude measurement is based on a defined reference datum such as mean sea level. Altitude is use for controlling the light source position in a scene. The default altitude set as 45 degrees (ESRI 2014).
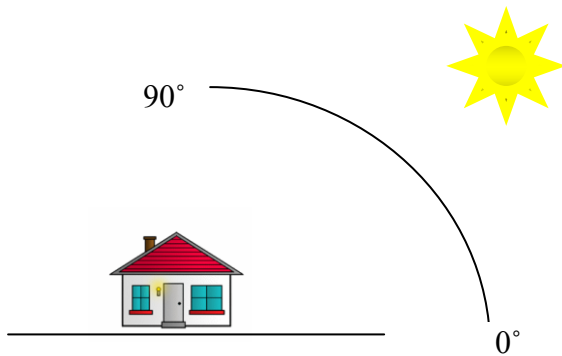
Figure 13: Schematic illustration of altitude illumination angle, units are in degree from 0-90

Hillshade is one of the tools in raster surface toolset which creates a shaded relief from a raster surface. For this work two different hillshade are made. First hillshade is of 315° degree angle whereas the second hillshade is for 45° degree angle. Two hillshade are used to ease the visualization of bedrock structures trending in different directions to minimize visual bias (Smith and Wise 2007). For both hillshade models, altitude is set as default which is 45 degree.

2.5 Digitization of Bedrock Fractures

The proposed approach of this master thesis is to work on a small area to extract bedrock lineaments and fractures. There are many ways to extract lineaments and fractures from maps. For this subject, it has been decided to digitized bedrock structures manually by digitizing from shaded relief from high resolution DEM.

Digitizing is process of converting analog spatial information mainly maps to digital format. The process involves drawing and recording spatial features with the help of a digitizer or a device similar such as a mouse whereby the x, y coordinates of these features get automatically recorded and stored as digital spatial data together with attribute tables along (Peuquet and Marble 2003, ESRI 2014). In GIS, digitizing could also be considered as a technique that produces vector data in form of points, lines and polygons. In order to visually interpret the bedrock structures in the two hillshades, polylines were used to digitize the connectivity of the pathways. The digitizing process started by creating new polyline feature class in a geodatabase within ArcCatalog application, and then adding the created feature class as a layer to ArcMap 10.1. The following simple steps were followed in the digitizing process;

1. Creating an empty shape file
2. Adding a new file in attribute table
3. Digitizing fractures and entering tabular data

Most bedrock fractures were visible in the 315 degree hillshade. However, some additional fractures were found in the 45 degree hillshade. The aim of manually digitizing the bedrock lineaments was to as accurately and unbiased as possible map the distribution and properties of bedrock lineaments in the test area on Bømlo.

2.6 Assessing lineament connectivity (fluid flow pathways)

There are several types of measuring options available in GIS for measuring distances between spatial points. Depending on which application is used the measuring metric could be different given the users' interest (Longley 2011). In this study, the Euclidean distance or Euclidean metric or straight-line metric option was used to measure the distance of connectivity pathway between points. Using a simple measurement tool, only the visible connectivity pathways were measured .This operation aimed at determining the shortest distance between the given points as shown in table 2 and 3.

2.6.1 Manual calculation of fluid flow pathways

The main objective of this method is to find the most obvious and connected pathways from the created hillshades with bare eyes. Normally it is easy to draw the desired pathways since the area is not big and the resolution of the raster is so high and most paths are clear. Two methods have been used here. They are not very different, but they do have a small difference in precision.

This method is easy and simple way for finding fluid flow pathways. It is like a labyrinth that the aim is to find the best and connected path of bedrock. The work has been done on hillshade layers, both 315 and 45 degree. All pathways have a start point and an end point. The consideration is to draw the most connected path, i.e. the shortest and most efficient path between the start and ending points. Afterwards measurement was done with ruler tools in Arc Map toolbar.

2.6.2 Automatic calculation of fluid flow pathways using network analyst

With this method the main idea is to find the best, most efficient and shortest pathway between two desired points. It is assumed that this method will help to find the connected structures automatically with the using digitized fractures as input. As it is automatic it aims at saving time with large datasets.

2.6.2.1 Network analyst

The Network Analyst extension in ArcGIS helps to construct a network dataset and carry out analyses on a network dataset. A network is made up of edges and nodes, edges are assumed as ''lines'' in the network system and nodes are physical locations. For this case edges are the digitized lines. And nodes are start point, end points and vertices in each route. The network analyst procedure is as follows:

1. Creates network analysis layer
2. Adding network locations
3. Sets analysis properties
4. Performs, solves analysis and displays results

In 1963 a "network" was defined by Kansky as a set of geographic locations interconnected in a system by number of routes (Kansky 1963). Normally a network consists of lines which can help to provide the spatial concepts of distance and connectivity (Yeung and Lo 2002) By using network analyses application in ArcGIS many spatial questions about linear networks could be answered (Comber, Brunsdon et al. 2008). An example of such question is what is

the connectivity between given points? This is because it gives the appropriate route, which is time saving and in large and complex datasets aids in the decision making process. In GIS, this is a basic task for different applications such as hydrology, transportation engineering, business and service planning (Jiang and Claramunt 2004). Five elements are basics in network analyst: links, turns, stops, centers, and barriers. It is not mandatory that in each process in network analysis all five elements have to be presented (Djokic and Maidment 1993).Network connectivity aims to define the way that lines and points connected to each other (Childs 2005).

2.6.2.2 *Feature to line Conversion*

Feature to line conversion function helps to create a feature class splitting lines at their intersections points (ESRI 2013). Digitized lines were used as input data for this process. Therefore, as figure 11 shows, "feature to line conversion" applied on the original digitized lines. Thereafter, the intersected points of the digitized lines get new vertices that originally were not detected. This operation is necessary to run the network analysis and connectivity between pathways. Network analyst solvers read input from and write output to, network analysis class (ESRI 2014). In network solve the goal was to find the best connected path ways within the bedrock fractures. Each time just 2 stops were used whereby stop 1 was the start point and stop 2 was the end point. Figure 14 shows how lines can be split at their intersections.
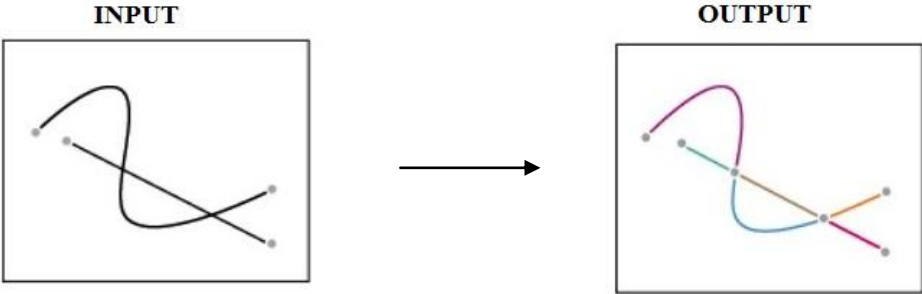
Figure 14: Line splitting by Feature-to-line function, illustration modified from (ESRI 2013).

2.7 Calculation of Saprolite Volume

To calculate the surface volume in ArcScien it was necessary to have a Triangulated Irregular Network (TIN) layer. A TIN surface can be created from a raster or terrain datasets. Therefore the TIN was made from converting DEM (raster surface) using the *"Raster To TIN"* geoperocessing tool.

2.7.1 3D analyst

While every feature in the real world is in three dimensions understanding phenomena in 3D is easier than 2D. Lots of questions could be solved during a 3D view of an area or phenomena and perhaps many questions could have an answer by 3D view as well. For instance, a study of the issues of how large a volume of Saprolite could be presented in an area can be determined with 3D analyst? If we blast away the 30 meters of either down the hills or top of hills, how much Saprolite could be there? Such question can be solved by using 3D analyst in ArcGIS. In 3D analyst there is possibility to calculate parameters for the area and volume of the surface (Longley 2005, ESRI 2013).

2.7.2 3D terrain visualization

The 3D mapping and 3D visualization techniques and output results greatly help to understand and interpret data. 3D visualization is one of the most exciting tools and application in GIS technology. Three dimensional terrain modeling is a way to demonstrate digital version of the scene that is observed by a viewer in physical real world (Yeung and Lo 2002). The last part of the practical work in this study is in Arc Scene. The 3D model of the study area is used to calculate hypothetical saprolite volumes at different defined elevations. In general it is necessary to have ArcScene; TIN layer derived from 1 meter resolution DEM, surface volume tool, and a reference plane. In 3D analyst toolbox, under functional surface, the surface volume tool was used. Although this is possible to work with 3D data in 3d analyst such as raster and 3D features, here definitely the input of this calculation as we mentioned earlier should be a TIN layer.

2.7.3 Reference plane

The volume and area under the plane in relation to the TIN surface can be calculated either above or below the defined elevation plane. The Reference plane used in this calculation was ''*below''* option. The aim was to calculate the thickness volume of layers between two different elevations. Different *plane height* which is used to calculate area and volume was set. The Z factor used for converting z-units to match with XY units was set to 1. The Output

file in notepad format was obtained for each calculation. This output of the surface volume calculation included information such as; Dataset, Plane Height, Reference Plane, Z-Factor, 2D area volume in square meter, 3D area volume in cubic meter. Figure 15 presents the volume calculation scenario of a surface area above or below a reference plane.
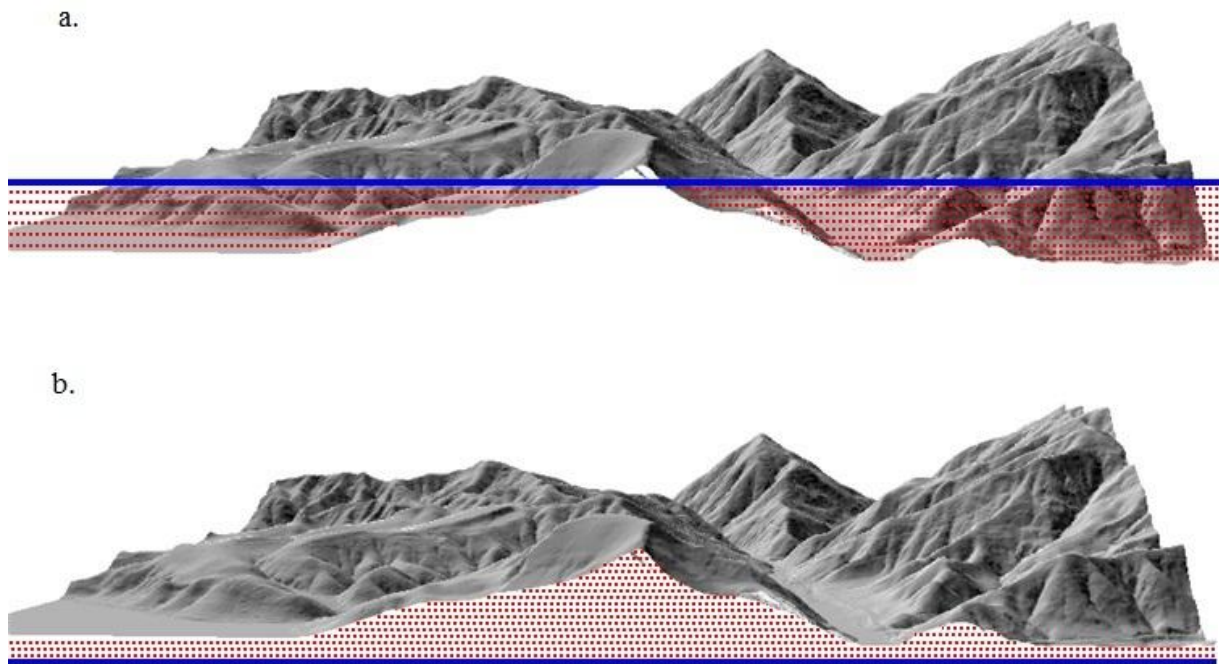
Figure 15: Illustration demonstrates the surface volume calculation. In (a.) the reference plane is set as "below". In (b.) the reference place set as "above". The figure is modified (ESRI 2012).

3 Results

3.1 LiDAR Digital Terrain Model (study environment, scenario)

Figure 16 shows an overview of the whole area where study area is extracted from. The map is derived from LAS files of LiDAR Data for Bømlo Island located south-west Norway. In order to test the proposed hypothesis without loss of generality we limit the study area to a 1 x1 km (1km^2) sample area. The selection is random and it is done only to reduce the processing load and study complexity. The highest point in the clipped area is 141 meters whereas the lowest point stands at 21 meters above sea level. The peak is located the east side of the study area. The area contains steep slopes on the east side while on the west side the topography becomes undulating from the valley.

As referred in the methodology chapter (section 2.2) we confine the study only to the DEM data from LiDAR. DEM excludes vegetation thereby showing only the bare rock surface and in this study it acts as a basis for preparing the Hillshade, Filtering and Triangulated Irregular Network (TIN). Furthermore, the LiDAR derived DEM offers a higher resolution which is important for extracting bedrock fractures.
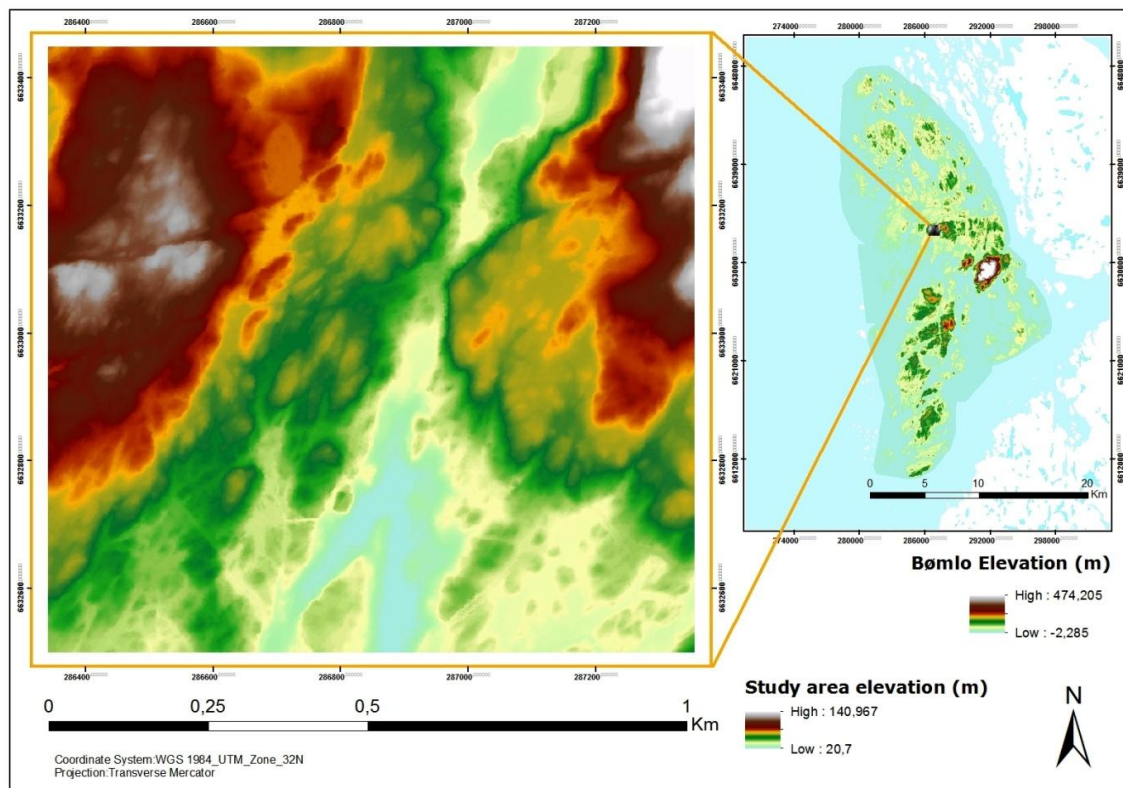
Figure 16: Digital Elevation Model and location map of the study area.

3.2   Filtering Methods

Edge detection and feature extraction is widely studied subject in image processing(Gonzalez, Woods et al. 2004). On the other hand, the edge detection in ArcGIS is executed using high pass filters. In the following subsections we test the output performance of different high pass filters for the sample DEM data.

3.2.1   Convolution functions

First, three different edge detectors are applied to the raster data (DEM data). To apply these filters ArcGIS executes a convolution functions on the DEM data, therefore the filters are referred to as convolution filters in ArcGIS. The three applied functions are some of the most common and recommended edge detecting filters for DEM. Matrices of the filters are presented in the section 2.4.1.1 and figure 11.

Each edge detector filter is applied in two variations: Sharpening and Laplacian filters are applied in two window sizes (3x3 and 5x5), and Sobel filter is applied in vertical and horizontal modes. Figures 17 and 18 present the results of six different filters applied to the original DEM raster data.

Sharpening 3x3

Figure 17 (a.) and figure 17 (a.a.) present the result after applying 3x3 Sharpening filter while figure 17 (a.a.) is only the zoomed version of the prior. The result of 3x3 sharpening filter is not significantly different from the original DEM data. No notable line detection is presented. No details are visible figure 17 (a.a.) and the raster image is blurred and unclear.

Sharpening 5x5

Figure 17 (b.) and 17 (b.a.) portrays the results for the same scenario as section (3.3.1), however for this experiment the window size is set to 5x5. Clearly this filter is not able to find bedrock edges. Similarly to the 3x3 case the zoomed raster image is also blurred and unclear.

Laplacian 3x3

Figure 17 (c.) and 17 (c.a.) shows the results after applying Laplacian 3x3 filter. In the result edges are sharp and small features stood out. However in zoomed-in version, it is not easy to see contrast between features.

Laplacian 5x5

Figure 18 (d.) and 18 (d.a.) portrays the results for the Laplacian 5 x5, however for this experiment it was expected the output was different compare to (section 3x3). Clearly this filter does not improve edge detection in an observable way. In the zoomed case raster image is also blurred and unclear.

Sobel Horizontal

Figure 18 (e.) and figure 18 (e.a.) show the results of applying the horizontal 3x3 Sobel filter to the DEM data. The images contain visible lines and edges and the features stand out. The horizontal alignments are clearer. In zoomed area of figure 18 (e.a.) relatively more details is visible. However ground features are still not very clearly defined.

Sobel Vertical

Figures 18 (f.) and 18 (f.a.) show the results of applying the vertical 3x3 Sobel filter to the DEM data. The image contains visible lines and edges and the features stand out. In this scenario the vertical alignments are more obvious. Figure 18 (f.a.) relatively more details and connectivity is visible. However the contrast is not significant enough for lineament mapping and connectivity analysis.

a.
Filter Type: Sharpening 3x3
Scale: 1:10000

a.a.
Filter Type: Sharpening 3x3
Scale: 1:2000

b.
Filter Type: Sharpening 5x5
Scale: 1:10000

b.a.
Filter Type: Sharpening 5x5
Scale: 1:2000

c.
Filter Type: Laplacian 3x3
Scale: 1:10000

c.a.
Filter Type: Laplacian 3x3
Scale: 1:2000
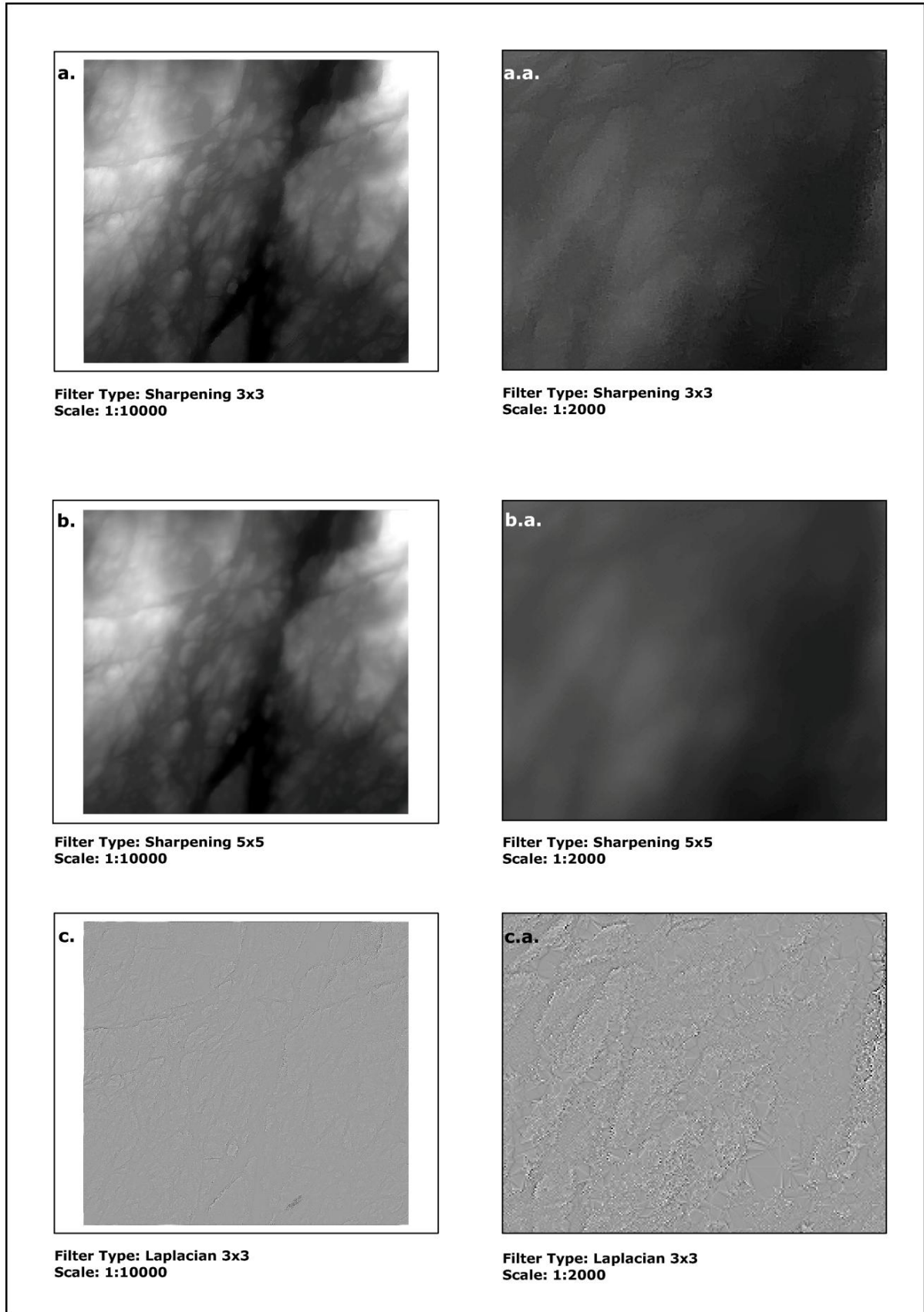
Figure 17: Convolution filter outputs for the study area. In (a, b and c) filters are applied on the study area separately. In (a.a, d.a and c.a.) a part of the study area is enlarged.

d.

Filter Type: Laplacian 5x5
Scale: 1:10000

d.a.

Filter Type: Laplican 5x5
Scale: 1:2000

e.

Filter Type: Sobel Horizontal
Scale: 1:10000

e.a.

Filter Type: Sobel Horizontal
Scale: 1:2000

f.

Filter Type: Sobel Vertical
Scale: 1:10000

f.a.

Filter Type: Sobel Vertical
Scale: 1:2000
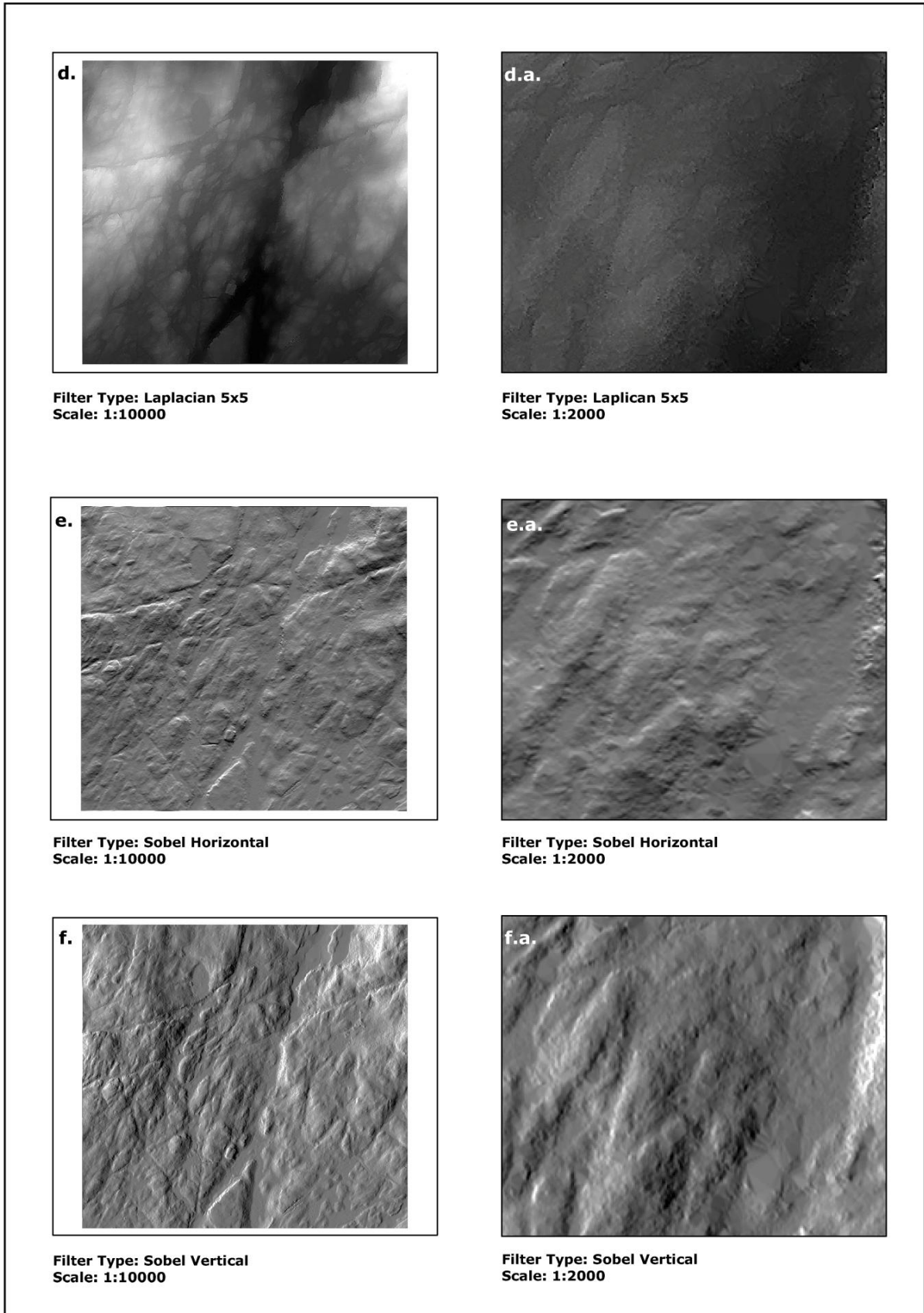
Figure 18: Convolution filter outputs for the study area. In (d, e and f) filters are applied on the study area .In (d.a, e.a and f.a.) a part of the study area is enlarged.

3.3 Hillshading Method

Hillshading of a terrain surface is one of the available methods in GIS for detecting linear features. In this model the terrain surface presents in grey scale 3D model, therefore depends on illumination source angle terrain relief will appear in a range of gray-shades.

Applying hillshade method on the terrain surface meant to shade the image with the according to a synthetically sun's relative position, this results in highlighting the surface features. In such model, shading from black to white depends on steepness of slope and how terrain is oriented towards the synthetically sun. Therefore, a slope that is faced against the sun is bright and a slope that is in opposite site and away from the sun is dark.

Input for this function is high resolution DEM. The azimuth properties which specify the sun's position are set to two perpendicular angles as 315˚ and 45˚. Figure 19 shows the results of the two different shaded reliefs. Since Sobel method proved to be the most effective convolution method, a comparison has been made between Sobel results and the hillshade results. The comparison is made for result raster images with 1:2000 zoom scale, and it is visible that hillshade method outperforms Sobel scheme. Therefore, in the rest of the chapter only hillshade results are used for facture digitization.
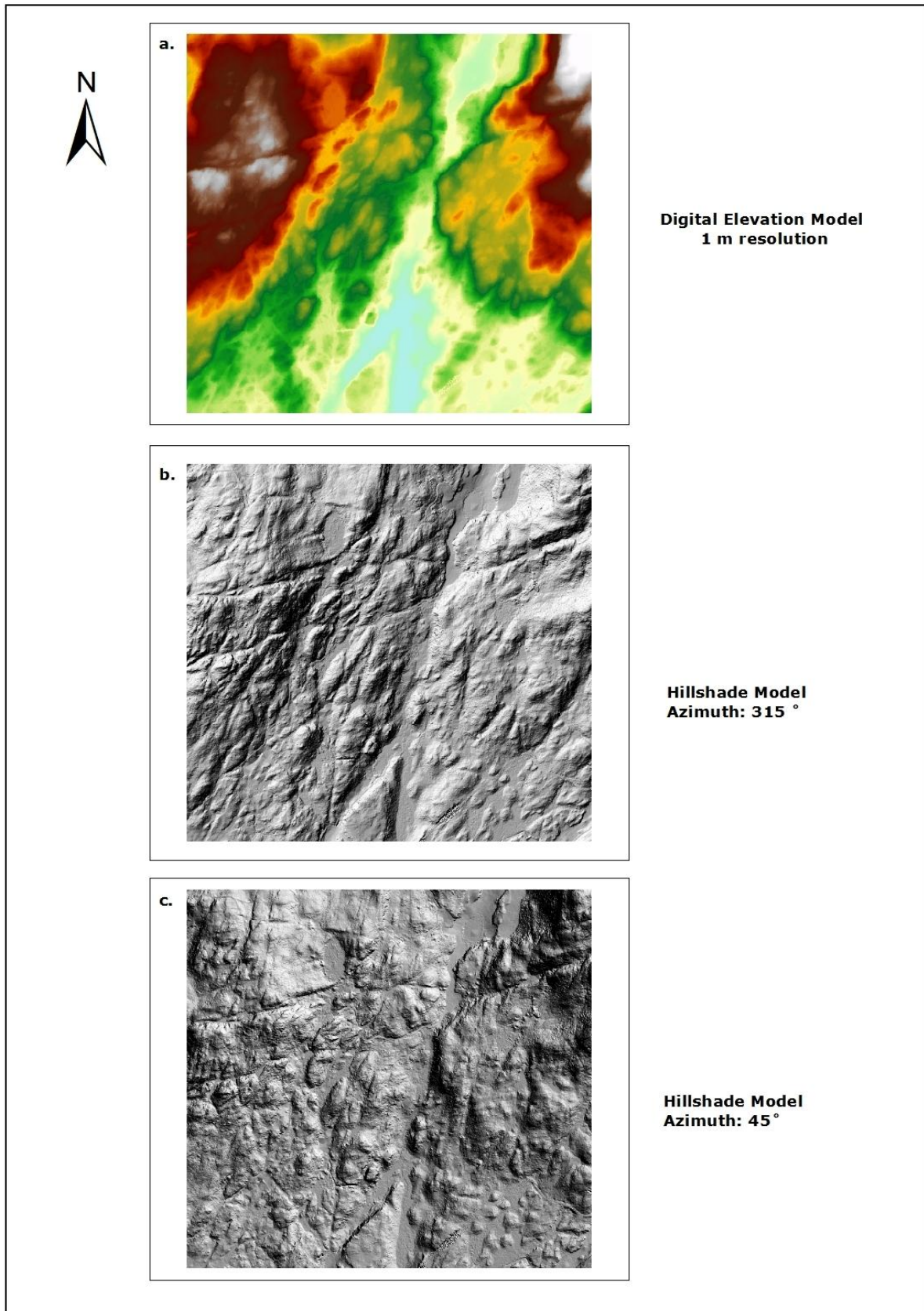
Figure 19: a) Digital Elevation Model of the study area (from top to bottom), b) Hillshade model of the study area with the default azimuth angle (315˚), c) Hillshade model of the study area with azimuth 45˚.

3.4 Bedrock structures

The bedrock structures are shown in figure 20. Based on the sun's angles, two different azimuth directions are generated. The two azimuth angles are named 315˚ and 45˚. For 315˚ the light source illuminates from Northwest direction and the latter illuminates in Northeast direction. Two directions are utilized for illumination, in order to reach a more visible bedrock fractures connectivity.

Illuminating from 315˚ and 45˚ enables viewing the structure from two perpendicular directions. For the cases that bedrock fractures lay in the same direction as one of the illuminations, naturally the resulting images cannot produce significant information. However, for such a scenario the other direction produces the maximum information because the lines are now perpendicular to the illumination direction. Therefore the extracted images from the two directions serve as two complementing data sources which should be superimposed. In Figure 20, the purple lines represent the lines extracted from 315˚ illumination source on the other hand the yellow lines represent the extracted fractures which are visible only from 45˚ illumination source, i.e. many purple lines could also be extracted using 45˚ illumination.
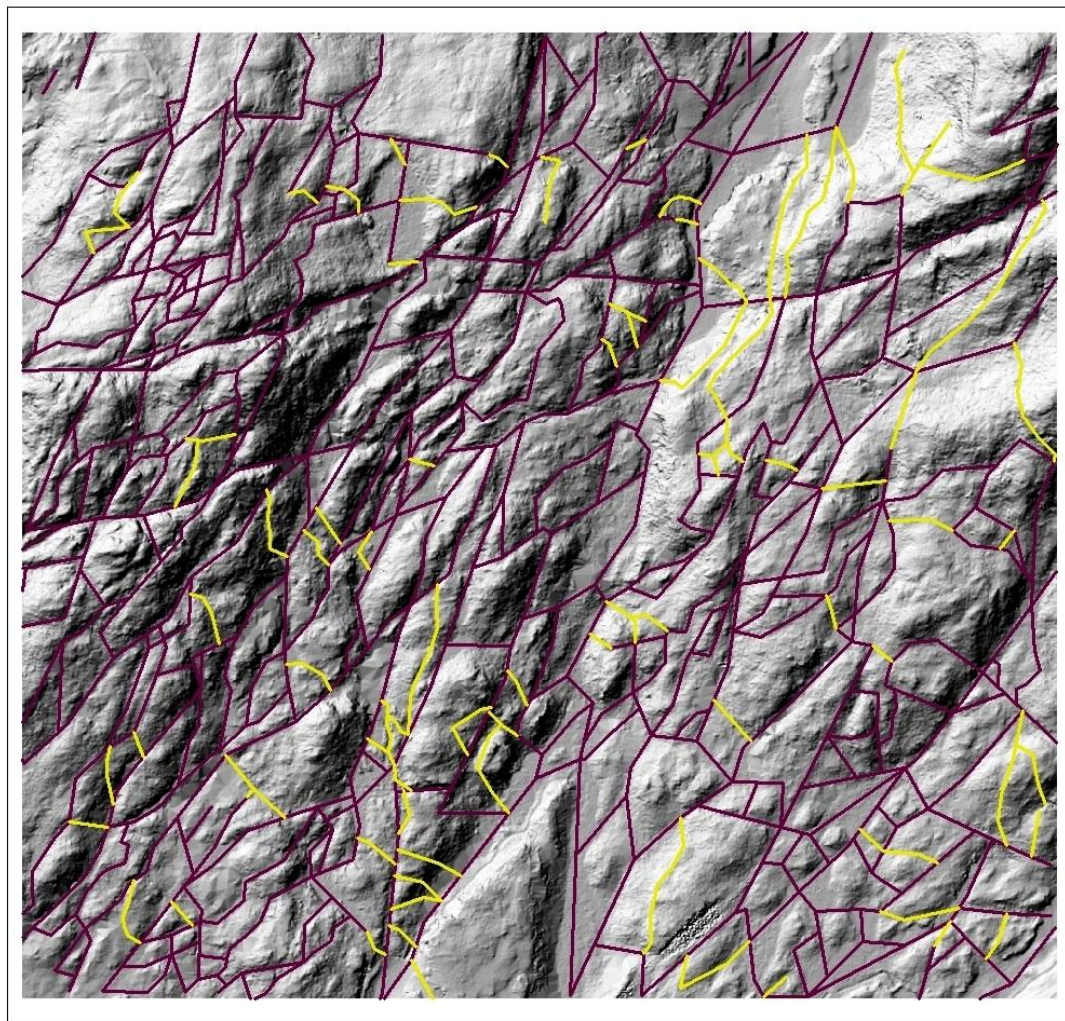
Figure 20: Extracted bedrock structure from two different hillshade azimuth angles (315˚ and 45˚).

3.5 Connectivity of Bedrock fractures

After detecting the fractures in section (3.5) the main goal in this section is to detect the connectivity and to measure the length of connected fractures. Finding the connectivity of bedrock fractures is of significance because it dictates the fluid flow pattern in the terrain. Two methods are utilized to estimate the bedrock fractures connectivity:

(i) Manual calculation (Drawing method)
(ii) Automatic calculation (Network analysis method).

3.5.1 Manual calculation of fluid flow pathways

In order to find the pathways manually, two nodes at the edge of the image is assumed, and the connecting pathway between them, which goes through a set of fractures, is traced manually. For the sample case of this study, twenty independent pathways are extracted from the bed rock structure. Figure 21 shows two samples of the selected pathways. The blue line depicts the traced connected fracture using the drawing tool in ArcMap and yellow line represents the straight line (Euclidian distance) between the two points. Table 2 is summarizes the descriptive statistics for the calculated pathways. Parameters in table 2 and 3 are defined as follows:

Euclidian distance is the length of the direct path between two destinations which is shown as yellow line in figure 21.

Fracture distance is the length the manually traced line between two destinations through bedrock fractures which is shown as the blue line in figure 21.

Length Difference is the subtracted value of the fracture distance and the Euclidian distance.

Length Ratio is ratio of the fracture distance to Euclidian distance.

Length difference percentage is the ratio length difference to Euclidian distance in percentage.

The median value for the length difference percentage is 6.5% for manual measurements, i.e. the manually traced fracture distances are 6.5% larger than Euclidian distance on the average.
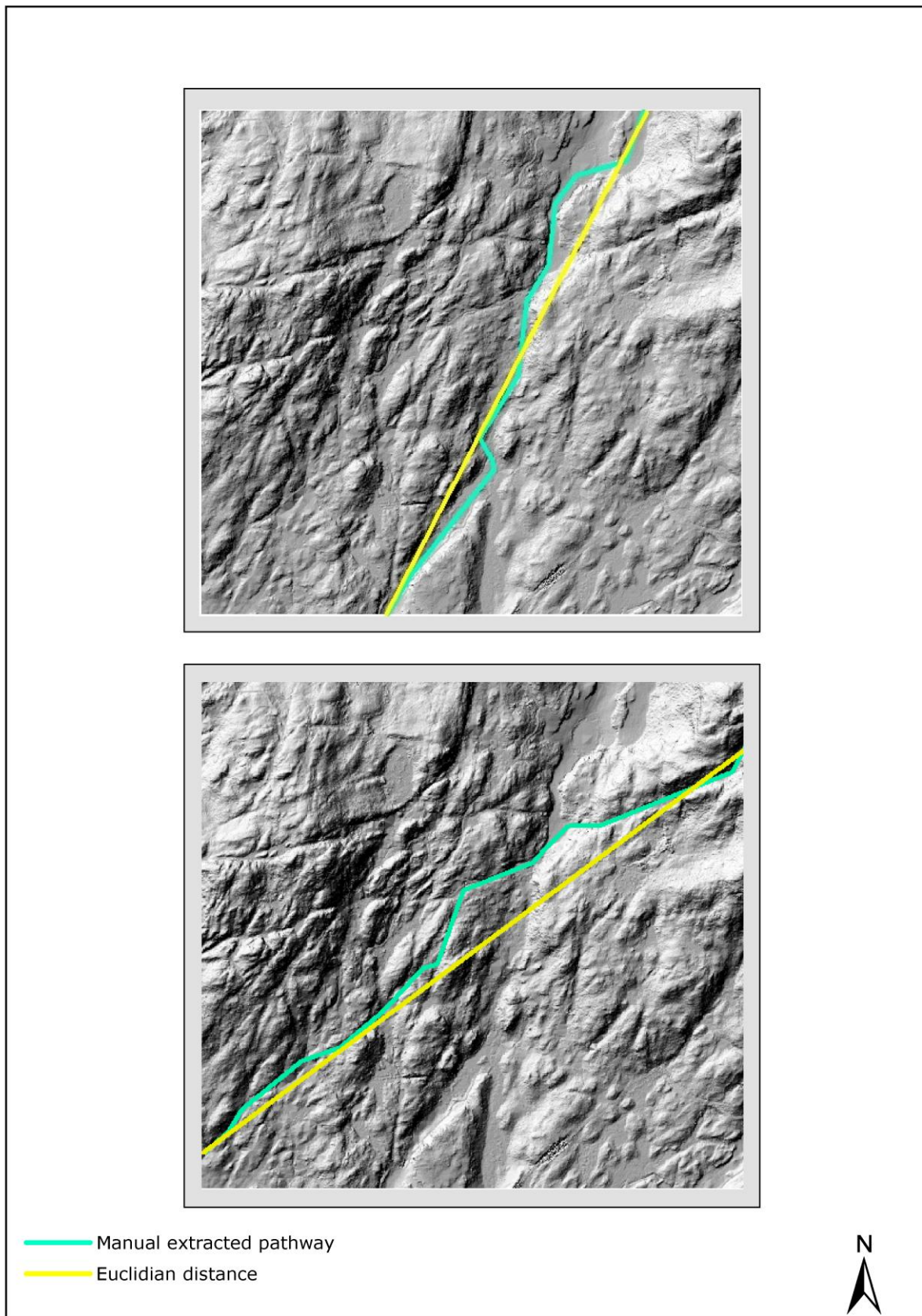
Figure 21: Manual pathway extraction, two samples of the twenty extracted pathways.

Table 2:Descriptive statistics for the twenty manually extracted pathways

Manually extracted bedrock fractures					
Pathway	Euclidian Distance	Fracture Distance	Length Difference	Length Ratio	Length difference percentage
1	1186	1370	184	1,15	15
2	940	1184	244	1,26	26
3	1010	1078	78	1,07	7
4	1338	1656	318	1,24	24
5	1069	1139	76	1,07	7
6	1057	1083	26	1,02	2,5
7	610	973	63	1,10	10
8	1024	1062	38	1,04	4
9	784	917	133	1,16	16
10	836	885	49	0,06	6
11	377	391	14	0,04	4
12	967	1024	57	0,06	6
13	1027	1064	37	0,04	4
14	954	1000	46	0,05	5
15	857	905	48	0,06	6
16	816	862	46	1,05	5
17	1257	1329	70	1,05	5
18	1007	1150	143	1,14	14
19	1249	1357	108	1,09	9
20	977	1118	141	1,14	14
MAX					26
MIN					2,5
MEAN					9,5
MEDIAN					**6,5**

41

3.5.2 Automatic calculation of fluid flow pathways by Network analyst

Network Analyst toolbox in GIS allows building a network dataset and provides network-base spatial analysis tools for solving complex routing problems. At the output, the toolbox provides a graph of edges and nodes, where the edges represent the bedrock fractures and nodes represent the intersection of the edges. The graph simplifies the potential fluid flow model within network. The most common network analysis is finding the shortest path between two points (ESRI 2012).

The digitized network from hillshade used as input for creating the graph data. In the derived network it is observed that in some parts there are no junctions at the intersected lines. In order to solve this problem, *"Feature to Line Conversion"* tool is applied to the network. This procedure assures that junctions are placed at the intersected lines. Figure 22 shows the network before and after applying "Feature to Line Conversion" function.

Subsequently, finding pathways within Network Analyst Toolbox is done similar to the manual method in section (3.7), where two nodes at the edges of the area are selected and the route between them is found through the network vertices automatically. This procedure is then repeated for twenty different pairs of edge nodes. As it is shown in table 3 for automatic extracted routes, ***fracture distance*** is automatically found as a part of route calculation. This parameter can be accessed from the "attribute table" for each route layer.

The median value of length difference percentage in this case is 7%. This number shows that the automatic traced fracture distances are 7% percentages larger than Euclidian distances.

The analysis of the extracted traces shows no significant difference between the two methods. The other major conclusion is that only by adding ***Length difference Percentage*** to the Euclidian distance it is possible to realistically estimate the actual path length.

It has to mention that generally the pathways length in the automatic process in NW_SE compares to SW_NE are longer. This act is due to the general trend in bedrock lineaments trending SW_NE creating natural connectivity in that direction, while the perpendicular NW_SE routes are more complicated and longer. Figure 23 shows the mentioned difference that SW – NE has straight pathway and NW – SE is complicated.
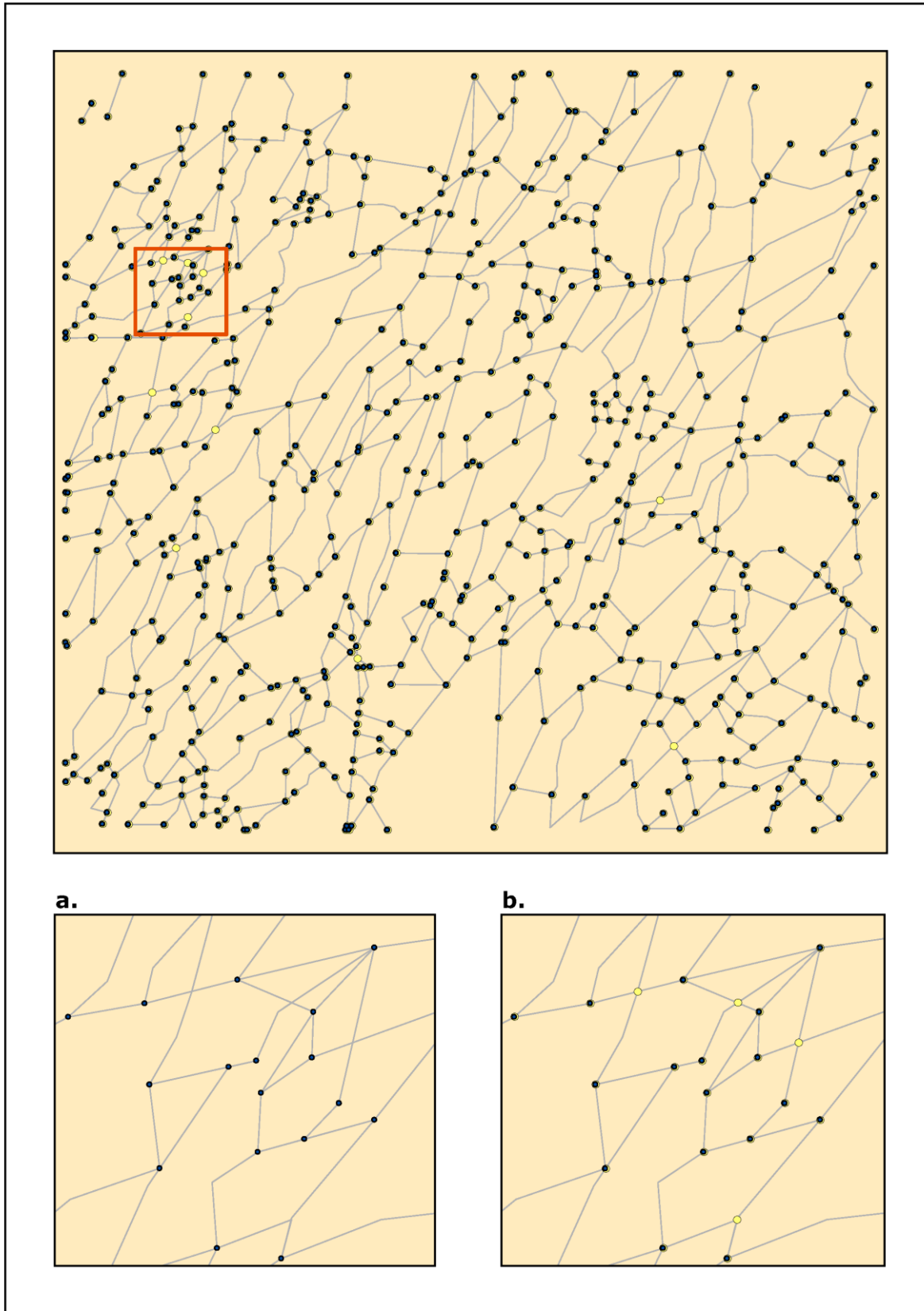
Figure 22: Feature to Line Conversion function, main map presents the result of applying "Feature to Line Conversion" to digitized lines (bedrock structure). The red box refers to the inset maps below, (a and b). (a.) shows lines before applying the function, (b.) shows split lines and new junctions at the intersected area.
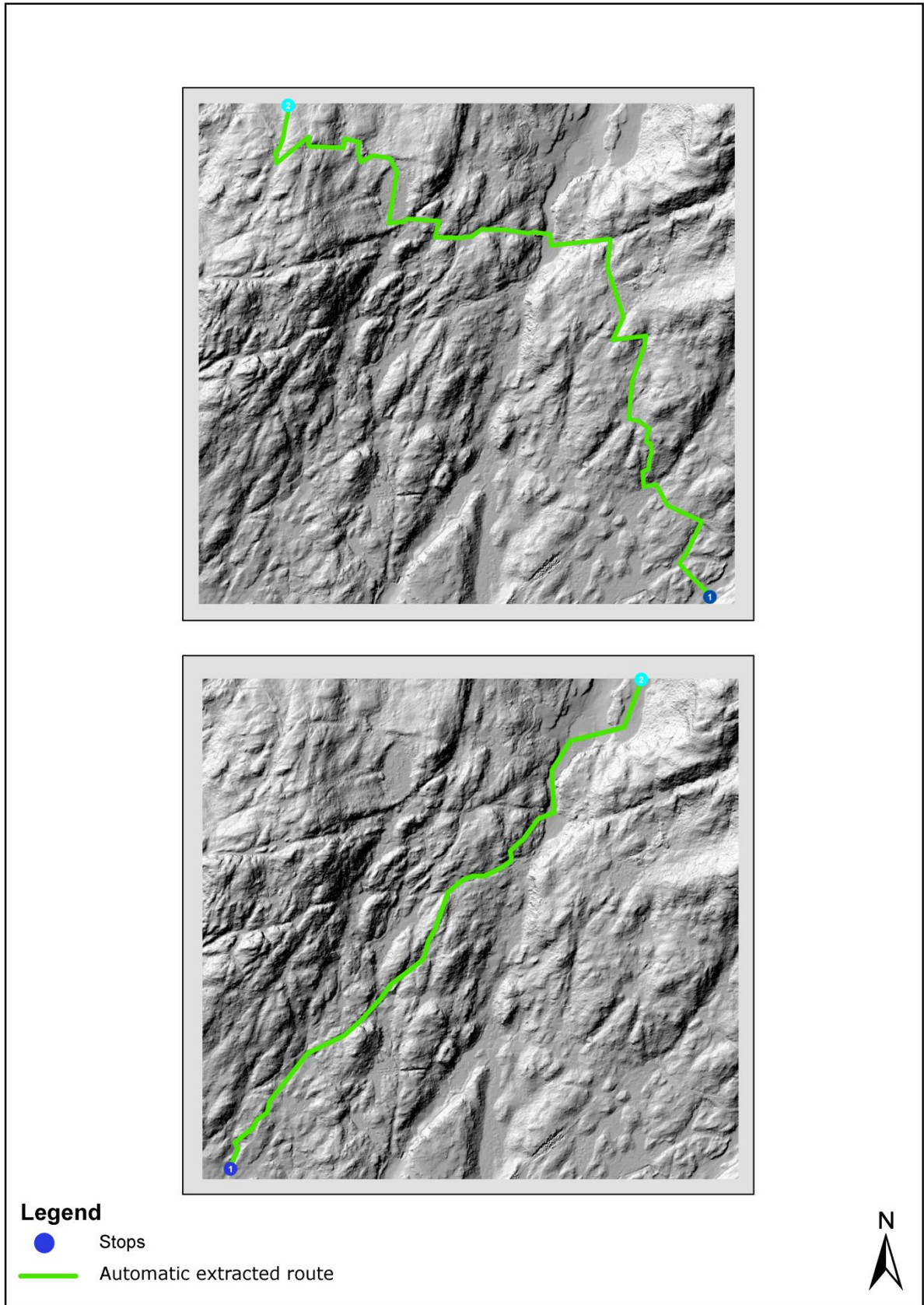
Figure 23: Automatic pathway extraction, two samples of the twenty extracted pathways. The blue dot depicts the start and end points. The green line between two points is the automatic detected pathway.

Table 3: Descriptive statistics for the twenty automatically extracted pathways

Automatic extracted bedrock fractures					
Pathway	Euclidian Distance	Fracture Distance	Length Difference	Length Ratio	Length difference percentage
1	1050	1099	49	1,04	4
2	1226	1313	87	1,07	7
3	1186	1256	79	1,06	6
4	1016	1290	274	1,26	26
5	1057	1119	62	1,05	5
6	800	856	56	1,07	7
7	1011	1360	349	1,34	34
8	1105	1340	235	1,21	21
9	515	548	33	1,06	6
10	260	287	27	1,10	10
11	555	714	159	1,28	28
12	325	356	3	1,09	9
13	437	667	230	1,52	52
14	1055	1105	50	1,04	4
15	590	637	47	1,07	7
16	580	654	74	1,12	12
17	969	1024	55	1,05	5
18	701	750	49	1,06	6
19	896	933	37	1,04	4
20	567	611	44	1,07	7
MAX					52
MIN					4
MEAN					13
MEDIAN					7

3.6 Saprolite volume and corresponding pore volumes

Hypothetic volume of saprolite in the area is calculated with the *Surface Volume* function in ArcMap. This function calculates the mass volume of the surface above or below a certain reference plane. The term of *mass* refer to the volume of saprolite that has been eroded away in the study area. The inputs to the function are the plane definition, TIN data and the desired orientation (above or below). At the output the function calculates the mass for located above or below the plane cross section. In the current study, the orientation parameter is set in order to calculate the mass (eroded saprolite) below the cross section.

Table 4 presents the results of surface volume calculation for 15 planes with different elevations. The lowest and highest points in study area are located at 21m and 140m respectively. Accordingly the lowest and the highest plane heights are set to 25m and 150m. Figure 24 represents the surface volume calculation of the study area in 3D for three example planes out of 15. For the sample figures the orientation is set to below and the plane height is set to intersect the surface at minimum (25 m), medium (70 m) and maximum (150 m) elevation.

For calculating of probable available saprolite in study area it is essential to have volume surface in cubic meters. Therefore the numbers which are used for calculation are the third number group of surface volume dialog box, which is called ''Volume'' in cubic meters.

Porosity of the bedrock crystalline in Norway is estimated to be approximately 25% (Olesen, Bering et al. 2012). Therefore all calculated volumes are multiplied by 25% to estimate pore volume in each of the investigated scenarios within the study area.

Table parameters in the table 4 are defined as follows:

Plane Height: The height of the horizontal reference plane from which calculation is derived.

Volume: The space between a reference plane which is set at a particular height and the surface in cubic meters.

Porosity: is porosity of saprolite soil in Norway that is assumed to be approximately 25%.

Pore Volume: is *"Volume"* multiplied to saprolite *"porosity"*.

Legend

TIN Elevation Values

	128 - 141
▨	114 - 128
▨	101 - 114
▨	88 - 101
▨	74 - 88
▨	67 - 74
	34 - 47
	21 - 34
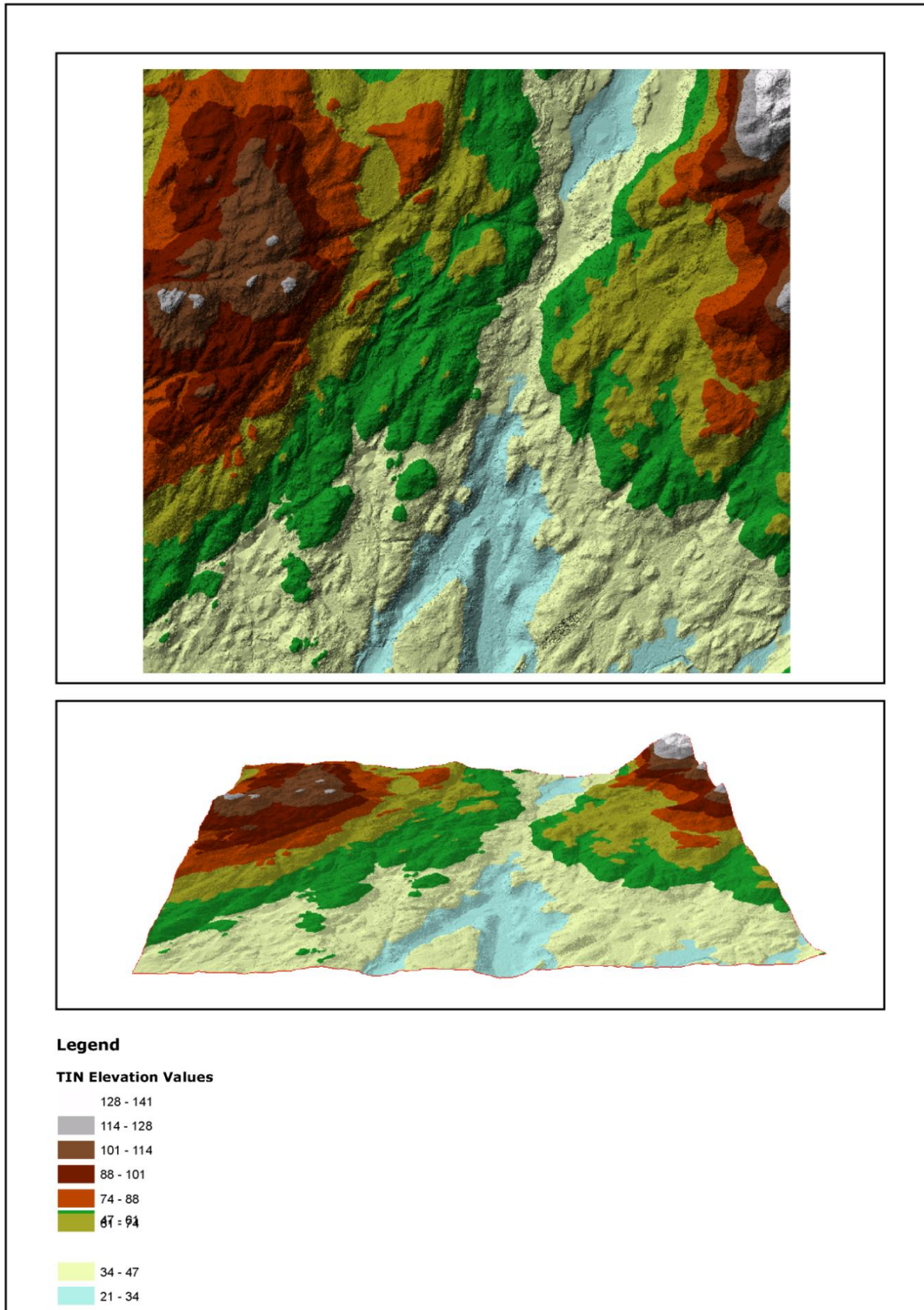
Figure 24: Triangulated Irregular Network surface (TIN) of the study area as an input for *Surface Volume* function.
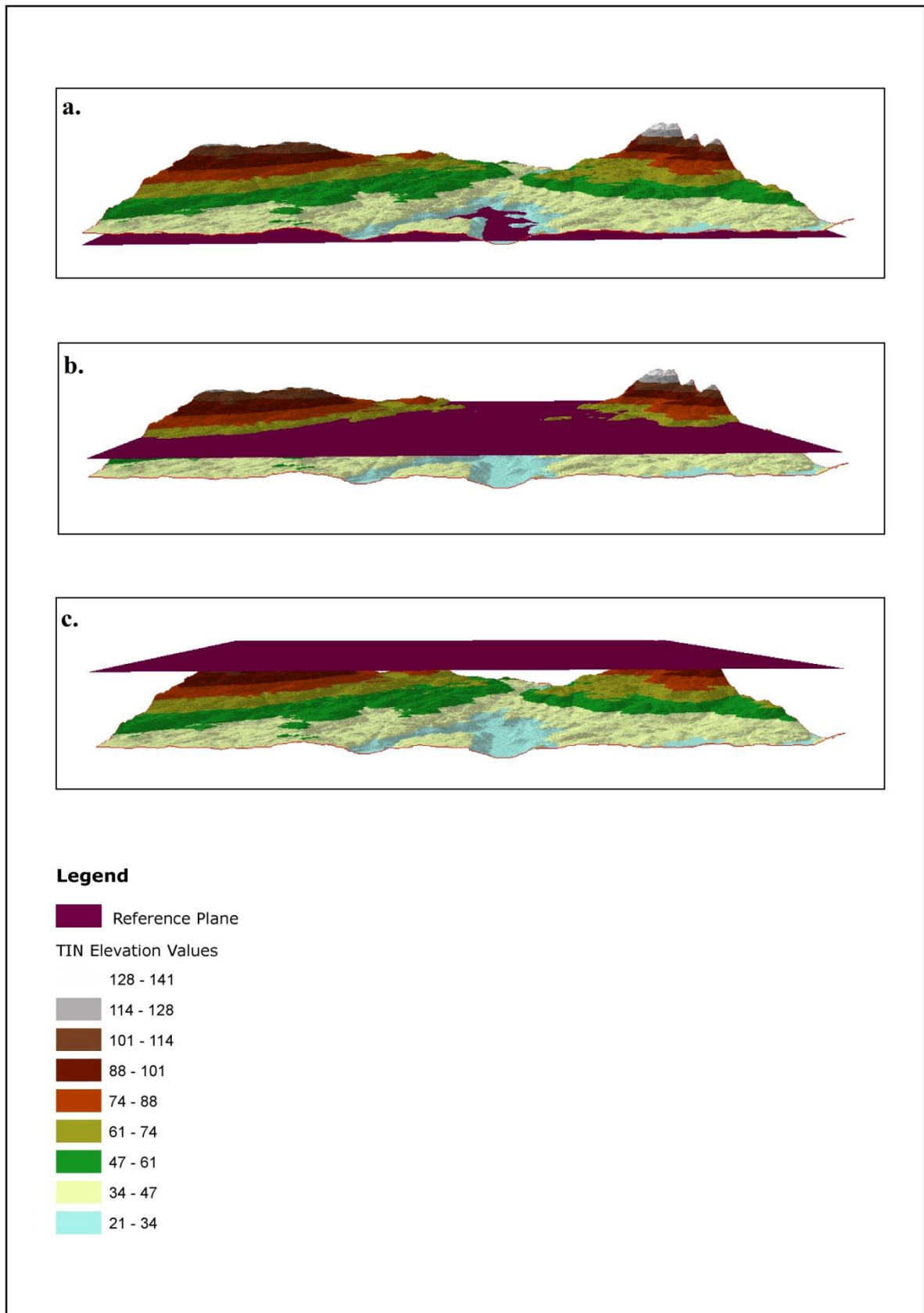
Figure 25: The surface volume calculation of the study area in 3D for three example planes out of 15. The reference plane set as below, a.)minimum, b.) medium , c.) maximum scenario.

Table 4 :Surface volume calculation results for 15 different planes elevations

Surface volume			
Plane Height (m)	**Volume (m³)**	**Porosity (%)**	**Pore volume(m³)**
25	7,0E+04	25%	1,7E+04
30	2,5E+05	25%	6,3E+04
35	5,9E+05	25%	1,5E+05
40	1,4E+06	25%	3,5E+05
50	4,5E+06	25%	1,1E+06
60	9,1E+06	25%	2,3E+06
70	1,5E+07	25%	3,8E+06
80	2,2E+07	25%	5,6E+06
90	3,0E+07	25%	7,6E+06
100	3,9E+07	25%	9,7E+06
110	4,8E+07	25%	1,2E+07
120	5,8E+07	25%	1,4E+07
130	6,7E+07	25%	1,7E+07
140	7,7E+07	25%	1,9E+07
150	8,6E+07	25%	2,2E+07

4 Discussion

This section discusses the outcome of using high resolution LiDAR data to map bedrock lineaments, understand fluid flow pathways and soil volume in a landscape in western Norway. The derived terrain models used in this study calculate the connectivity of deep-weathered bedrock is scrutinized together with the suggested model for the hydrocarbon/groundwater reservoir in eroded saprolite in Bømlo area. In addition, the research questions will be discussed along with implication of this study and a comparison with other studies. Finally the limitations of the study are underlined and directions for the future work are also presented.

4.1 Lineament mapping and Interpretation of LiDAR derived elevation model

The first objective of this study is to find connectivity and pathways in a small scale area (1km^2) almost at the center of Bømlo landscapes. To achieve this goal different ways of processing the LiDAR data were tested so that manual digitization of bedrock lineaments would be optimal. As Figures 17, 18 and 19 show, 8 different edge enhancement techniques were applied on the 1 m resolution DEM. The outputs of only 2 methods were selected for processing in the next steps (hillshade models). The other 6 methods outputs (Convolution filters images) were excluded due to undesirable results when the images were enlarged. However, such exclusion cannot be generalized to other datasets. It means that those 6 excluded methods might be efficient in other cases; e.g. when the study area is very large and the scale of the images is small. Hence, a close scrutiny of the results of different filtering methods is a necessary step to enhance the visual signature of lineaments. Such an enhancement facilitates mapping the extracted lineaments. This process is important to find out which methods are efficient for different DEMs.

Hillshading, using two different synthetic illumination was found to be the most consistent and straightforward method to enhance bedrock lineaments, that allowed easy manual mapping of the most significant bedrock lineaments. Bedrock structures for an area of 1km^2 in the center of Bømlo Island in south-west of Norway have been extracted from the 1-m resolution DEM derived hillshades. The mapped fractures were then used to calculate the connectivity between fractures and potential fluid flow pathways. At the same time, the high quality hillshades demonstrate that the landscape of study area is deeply-weathered and fractured. In figures 20 and 22, it is clear to see that lines have intersected with high frequency, especially in north-west and south-east of the area.

To find connectivity between fractures and calculate fluid flow pathways, manual and automatic methods were applied and compared to each other.

In manual pathway extraction, among 20 random pathways, the maximum *length difference* is 26% longer than Euclidean distance while in minimum scenario it is 2, 5% longer. Finally the median of the measured distances is 6, 5% which cannot be considered as a significant difference. The obtained pathway distances show that potential fluid flow pathways are short and fractures connectivity is high.

For the automatic method, 20 pathways (almost with the same direction of extracted manual pathways) extracted as well. In this method, the maximum *length difference* is 52% while the minimum is 4% longer than the Euclidean distance. To conclude, although the difference of maximum and minimum length is high in automatic pathway detection, the calculated median is just 7% longer than the Euclidian (shortest) distance.

The comparison of two methods shows that while the required time to conduct the automatic method is much less than the manual method, the efficiency is not significantly different. There is no large advantage in using automatic pathway calculation for this small dataset. However, with much larger datasets (for example thousand of mapped lineaments), it is possible to get more reliable results faster with automatic connectivity calculations. It should also be noted that manual digitization of the bedrock structure has to be done before applying the automatic method (Network Analyst).

Then, results from this part can answer the first research question of the study:

1. What are the connectivity and pathways in the study area?

According to the bedrock structure digitizing process and the obtained median of two methods, it is concluded that the connectivity of the weathered bedrocks in the study area is high and pathways distances are short.

4.2 Surface Volume and Interpretation

In this section, the second and third research questions will be answered and discussed by explaining the hypothetical scenario of eroded saprolite. Consequently the potential volume of fluids (oil or water) based on a standard porosity is calculated.

4.2.1 Saprolite Volume

To calculate the potential volume of saprolite, a hypothetical scenario is developed in ArcMap to measure the surface volume. It is important to note that in this study saprolite refers to eroded away soil which most likely belongs to the Plio- to Pleistocene time periods, but it is still present in the offshore landscape and source. The estimation of saprolite mass in the exposed area is a key conduit for predicting the storage of resources. The thickness of chemical weathered saprolite in Norway is quite varied. Through the geophysical research that has been made in different places in Norway e.g. Oslofjord region, the thickness of saprolite layer has been measured up to 100 meters (Olesen, Bering et al. 2012). There is some evidence showing the affect of deep weathering on some parts of Bømlo's landscape (Gunterberg 2013). Faults and fractures of the area are filled with thick layer of saprolite. Therefore, calculating the amount of saprolite in fractures pocket is important. In this part for calculating the amount of saprolite mass, as figure 25 shows, the mass below the cross section is estimated for different layers.

In the minimum calculation scenario, the plane for cross cut has been set at 25 meters, just 4 meters above the lowest point of the study area. Since the cross plane is set so low, only a "pocket" in that specific location (lowest point) will form, see part (a) in figure 25. As a result, estimated saprolite volume in the minimum scenario is 70,000 m^3.

This calculation has been done for 15 other cross planes to estimate the mass of saprolite layers up to 100 m above the lowest point. The last plane was defined assuming that all the area is buried by weathered saprolite.

The depth of saprolite varies all around the world, but within certain limits. For instance it is observed in northwest of Portugal (Braga, Paquet et al. 2002) that saprolite layers are around 10 m or more, while in other places such as Burkina Faso in Africa it varies between 10 to 100 meters (Sharp 2014). Through geophysical studies of saprolite layers in Norway the thickness of saprolite in Kjose (Vestfold) and the Oslofjord region reach almost 200 m (Lidmar-Bergström, Olsson et al. 1999). Also an observation in Scania reports 60 m saprolite thickness (Gunterberg 2013). However, these cases can be considered as the most extreme

scenarios. Maximum scenarios average saprolite thickness in Norway is much less. By looking at the study about saprolite distribution in Burkina Faso, the common average heights of saprolite layers are be between 20 to 40 m (Sharp 2014). Assuming that the lowest point is 21 m above present day sea level, the uppermost surface of the modeled saprolite is between 40 m to 60 m above present day sea level. The volume of saprolite at 40 m height is predicted to be 1, 4 million m^3 and at 60 m height is 9.1 million m^3 in a 1 km^2 area.

4.2.2 Saprolite Porosity

To assess the amount of liquids, hydrocarbons or water, than can be contained in a specific volume of saprolite, it is essential to know the porosity of saprolite. Unfortunately there is no available data for the percentage of porosity in Bømlo saprolite. Recent discoveries of saprolite porosity of the chemical weathering in Norway is measured at Vestvågøya in Lofoten with a porosity of approximately 25% (Olesen, Bering et al. 2012). Hence, to find out the saprolite pore volume, all the obtained saprolite volumes have multiplied by 25%. Table 4 shows the pore volume for all the modeled saprolite thicknesses. The pore volumes of saprolite layer at 40 m and 60 m height above present day sea level have approximately 350,000 m^3 and 2,3 million m^3 respectively. To give a sense to this number assumes the following example. According to U.S. Geological Survey, a human being consumes 36500 gallons of water per year (USGS 2014). So, the pore volume of a modeled saprolite with top surface at 60 m is 2, 3 million m^3 which is equal to 608,000,000 gallons. Thus, this amount of water can supply daily water consumption for 16657 persons per year.

Results from this part can answer the second and third research question of the study:

2. How large are the volumes of saprolite in the study area?

See table 4, *volume* column.

3. How large are the oil reservoir volumes in saprolite in this type of landscape?

See table 4, *pore volume* column.

4.3 Related Studies

As it was discussed earlier, the goal of this study is to find connectivity of bedrock fractures in Bømlo Island using LiDAR data to assist further research in the natural resource management study. Various articles, papers and reports have been published on the analysis of lineament extraction using different data types and applying several GIS methods. Applying the hillshade method for lineament extraction is not novel; it is one of the most commonly used landscape visualization method and is often used for mapping landforms and geological structures (Onorati, Ventura et al. 1992). Geological mapping is essential for efficient natural resource management strategies. In this study LiDAR and GIS are utilized to form the best possible geological background for decision making in natural resource (e.g. hydrocarbons, water).

However, to our best of knowledge, there are limited number works that have used high quality LiDAR data for bedrock mapping as a way to better understand bedrocks structures, fluid flow pathways and pore volume. These parameters are essential for an efficient management of subsurface natural resources such as hydrocarbons or ground. The following studies presented related works in different locations around the globe which use different approaches to study bedrocks structure and fractures. Even these few studies, have been conducted in other areas aside from Bømlo.

In a recent study by Sturtevant (2014) in New Hampshire, the aim was to revise the bedrock structural geological map using hillshaded LiDAR data. Sturtevant mapped features that had never been seen before during traditional field mapping, for instance in areas where vegetation was dense. Therefore, he reevaluated the distribution and character of previously mapped bedrock units. Additionally LiDAR-based remote linear feature measurements were compared with field based fracture measurements. However, Sturtevant extracted lineaments on a large scale and delineate bedrock controlled and glacially-controlled regions through landscape mapping. Moreover, he found the correlation level of joints through comparison of the remotely measured lineament sets and the field measurements. Sturtevant has done a complete and precise bedrock lineaments mapping on large scale. In his work all measurements and calculations are real since all of them are compared not only to previous bedrock maps but also to field works measurements. Considering the study by Sturtevant provides more inspiration for doing additional works on Bømlo island through LiDAR data and remote sensing techniques. It should be noted that in the Sturtevant study, bedrock connectivity and pathways distances have real measurements, while in this study the mapped

bedrocks have not been compared by a field work. On the other hand current studies present a framework for the reservoir management and hypothetical measurements for a made-up scenario. Moreover, there is no previous lineament extraction map available for the study area. Therefore, the extracted bedrocks structures map is the first one on Bømlo on a small scale.

(Zelazny 2011) also considers Lineaments mapping using remote sensing techniques to digitized lineaments on a large scale in central New York State. Image processing is used to enhance lineaments patterns to extract the fracture structures in the region. However, the author's goal as a geologist was to manually extract linear features using satellite images (ASTER) and DEMs. Then, all extracted linear features are combined with field investigation to assist in identifying potential spots for carbon dioxide subsurface sequestration.

Zelazny used different image processing technique to enhance the lineaments extraction such as shaded relief method with different illumination angles. The DEM resolution was set to 10 meters and there were no lineament pattern identification in small scale since lineament length were more than 1 kilometer. Thus, geological interpretation is not detailed. 10 meters DEM resolution does not allow having insight into the geological structures in the area, otherwise more geomorphologic features could be mapped using high resolution DEMs. Compared to the study by Zelazny, in this study high resolution DEM and the hillshaded image provide geology structure of lineament patterns in a small scale and insight into the geomorphologic features.

In Sweden, (Nyborg, Berglund et al. 2007) conducted a hydrologic model using LiDAR data and hillshade models to map bedrock fractures. In their study, lineament detection is made automatically by filters in order to evaluate the long-term safety of deep repositories for nuclear waste. Filters identified linear features of interval length 2.5 – 50m which is assumed as a detail measurement and checked by field work. It is noteworthy that using filters will save time and man power. However the type of filter and software used in the study is not mentioned. Although the study is done on small scale, no bedrock connectivity structures are provided.

It is not simple to compare the mentioned studies to current work because it is specifically dealing with the problem in Bømlo. Based on these related studies it is concluded that LiDAR data, GIS processing and high resolution DEMs are most suitable to map bedrocks structures and fractures connectivity.

4.4 Management implications and opportunities

4.4.1 Remote sensing as a management tool

Remote sensing technologies are capable of providing a framework to analyze natural phenomena. Accordingly they have the potential to be used as a natural resource management tool (Lang 1998). As an advantage, these technologies can provide data from a remote area in a short time, providing spatial, spectral and temporal data. In addition remote sensing technologies offer a verity of tools for manipulating the collected data (Sener, Davraz et al. 2005). Moreover, all the information can be geographically referenced (Longley 2011). Therefore, remote sensing science and the wide variety of its applications act as a helpful and universal tool for natural resource managers (Kennedy, Townsend et al. 2009). This study uses remote sensing along with a conceptual framework in a management process to assist decision-making. In general in this study, these three steps are involved in the management process using remote sensing data; (i) data acquisition, (ii) image enhancement, (iii) analysis and estimation.

For the first step, two aspects are of paramount importance: data captured time and image quality. The utilized LIDAR data of the area is quite new and the derived DEM has 1 m resolution, which is considered as really high quality topographical data. Such a high resolution enables detailed mapping of bedrock lineaments and thus enables high quality connectivity analysis and landscape modeling.

It is noteworthy to mention that operating LiDAR data in GIS needs special attention and involves consideration for input data adoptability, for example LiDAR data are not supported by all GIS versions. Fortunately ArcGIS 10.1, and later versions, support LIDAR point clouds and allows the user to access different types of datasets such as LAS files and terrain models. GIS users should recognize and use the right and relevant format of data with specific license and version. The significant outcome of LIDAR data are high quality DSM and DEM models which serve as the foundation for bare-earth studies in this work.

In the second step, raster image enhancement is necessary to produce images which enable easy detection and mapping of bedrock lineaments and hence better analysis of lineament connectivity. As the preferred image enhancement method, in this study the hillshade method was chosen because of its higher reliability as it is shown in figures 19 and 20.

In the last step, finding connectivity and volume of eroded saprolite in the bedrock fractures, the measured pathways utilized to estimate the level of outcrop connectivity. Because many connections were found during digitizing and the pathways median is calculated to be small, one can conclude that the studied area is strongly fractured and therefore bedrocks lineaments are well connected. Therefore if there exists no barrier inside porous of the eroded soil, such as common chemical (clay existence) and physical (sub soil compaction) barriers, liquid sources (hydrocarbon and ground water) can migrate fast and easily. As mentioned in introduction section, the onshore analogous to Bømlo has been stripped of saprolite, however many other areas in the world and offshore places in Norway have saprolite preserved. Considering that such dens fractured area is filled by eroded saprolite, the hypothesis of buried hydrocarbon resource can be realistic.

Natural resource managers, hydrologist and geologist can use the presented analysis and data for further study of monitoring or identification of test sites for exploring either hydrocarbon or ground-water resources in Bømlo Island and elsewhere.

4.4.2   LIDAR and GIS as management tool

Remote sensing and the Geographical Information System with their advantages have become very practical tools for monitoring and evaluating the earth surface and natural resources. The combination of remote sensing and GIS techniques finds a significant place in professional careers involved in studying, measuring and managing features on the earth surface. Many scientists in different fields can make critical decisions by relying on such techniques (Lang 1998). By using these methods, operators have the possibilities to monitor and manage natural resources in details based on the recently acquired remote sensing data. Additionally, utilizing different derived datasets extracted from these data (such as terrain models) enables the operator to define different sets of frameworks to design models. These models can later be used to understand the surface features without any direct contact with them. Consequently, developing methods and models by each person brings many different "what-if" scenarios which allow the user to consider a framework and a plan which has never been considered before. Different considered framework could assist investigating the object in several spatial contexts and finally can suggest the pros and cons of each framework (Lillesand, Kiefer et al. 2004).

Recently as LiDAR data have become more widespread, many natural resource managers thrive to apply such methods in diverse fields of studies. Utilizing LiDAR facilitates the

transition from the theoretical studies to operational and practical domain (Hudak, Evans et al. 2009). Many fields of research including geology, hydrology, coastal studies, geomorphology, forestry, and wildlife can benefit from such a technology due to its precise and high resolution topographical data. As it is indicated widely in the literature, using LiDAR data driven information makes decision making a simpler process (Kreylos, Bawden et al. 2008, Brock and Purkis 2009, Lane and D'Amico 2010).

As an example, in geology studies LiDAR data provides many advance capabilities to categorize the features in the earth surface mapping process. For instance it enables separating soils, sediments and bedrock structures from each other (Van Den Eeckhaut, Poesen et al. 2005, Dar, Sankar et al. 2010, Pavlis and Bruhn 2011). Similarly, in many large scale studies, high quality LIDAR data helps to distinguish bedrock fractures, lineaments and faults with more detail. Moreover, it is confirmed in a couple of experiments that high resolution DEM derived from LiDAR data can achieve a higher accuracy in detecting topographic features compared to other conventional methods (Liu, Peterson et al. 2005, Sturtevant 2014) .

4.4.3 Management of hydrocarbon or ground water

Natural resource management entails careful investigation of complex systems (Mallawaarachchi, Walker et al. 1996). Management of hydrocarbon resources is a complex problem as such resources depend on many influencing variables such as lithological, geology, biology, and climate. It took almost a decade of study by different geologist and geologic remote sensing service firms to proof that remote sensing could be useful in petroleum exploration (Vincent 1997). Petroleum and ground water exploration can be considered similar in respect that reservoir studies for both usually involve issues such as porosity, permeability, sedimentary stratum and fluid migration. In many countries ground water exploration projects becomes more successful when spots for extracting and drilling are guided by lineament maps (Sener, Davraz et al. 2005). Bedrock lineaments and their characteristics have helped significantly in providing information on movement, capacity and storage of groundwater (Rao, Chakradhar et al. 2001). Although the two resources are different in many respects mapping of the surface structure with using remote sensing is a common element for both types of reservoirs (Vincent 1997).Thus, migration and storage hydrocarbon modeling in eroded saprolite can be adjusted to model ground water storage too.

Surely, predicting underground resources from an office by collected data does not give a guarantee to make the exact decision. Therefore, the analyzed and obtained data can work as

first order information for further studies. In addition, depending on the study type the definition of primary and secondary information changes. In many studies, remote sensing and finding the proper exploration sites is essential at the very first step (Schoorl, Sonneveld et al. 2000, Thompson, Bell et al. 2001, Jain and Singh 2005). On the other hand, for some other cases field work and resource exploration has the priority while remote sensing techniques work as study complements.

For our work, the extracted data are considered as primary basis of reservoir exploration. In the next step of exploration, an area survey by an expert makes the decision making even more reliable.

4.5   Study Limitations

Although the outcome of this study is precedence for predicting onshore and offshore seepage of hydrocarbon reservoirs, this research is conducted in the field of natural resource management, not within the geology domain. Therefore, field work was not a part of the study as it is in geological investigations, such as those discussed in related work.

One of the major limitations of this study is the real amount of saprolite volume in the study area. Unfortunately, due to lack of knowledge about the past volumes of saprolite in Bømlo area, the best way to define the volume and respectively the porosity of saprolite in this study was to model the volume by using other relevant studies. Because of this, the volume of eroded-saprolite is set by estimates from other studies such as study by (Gunterberg 2013) on the comparison of crystalline basement rocks in southern Norway and Sweden.

As also mentioned before, there is no information about Saprolite porosity in Bømlo Island. Thus saprolite porosity is set by other studies such as the TWIN report, hence the saprolite porosity and pore volume was calculated based on data from other regions of Norway.

Another limitation of the research was with the scale of the study area, which was small due to time constraints. The studied elements are fractures which are around 1 kilometer. While investigating wider areas, linear features which are larger than 1 km are considered as lineaments. Therefore, the results of this study can be a starting point for evaluating the structure of small scale bedrock fractures. For evaluating the structure of the area in a larger scale, it is possible to map longer linear features. Generally, evaluation of this study probably cannot be a representation of whole Bømlo. The effects of scale in data and data processing are recognized as fundamental aspect of any research as well as in geoscientific studies.

Another limitation of the study lies in employing network analyst in the automatic pathways method. While network analyst is typically applied in areas like urban planning and road constructing, it is not very common in geological studies. In this study, network analyst was been applied without any defined features such as elevation, distance calculation cost, time and etc. due to lack of required data. So, if these data were available, the extracted routes in the automatic pathways method could be more prices.

4.6   Future work

There should be more studies about fractures for more precise evaluation of connectivity. We can could choose several similar areas in other spots of Bømlo Island and map the bedrocks structures and apply the same process as the method in this study for each region. This results in calculating mapped bedrock structures, the fluid flow range and the surface volume for each area. Calculating these parameters enables comparing the different study areas with respect to bedrocks structures and connectivity, fluid migration and capacity and finally provides a more precise map from the whole area for further investigations. Additionally, mapping the connectivity of lineaments of surface on a large scale (for example for whole Bømlo Island) can help provide a good overview about the whole area.

Filters and automatic lineament extractions methods on high resolution DEMs can also be included in the study. There are possibilities in GIS to define matrix for filters for edge enhancement which need more image processing and mathematical background. For smaller studies like this study, manual mapping using a hillshade is the most effective method. However, for larger areas, filtering and automatic lineaments extraction would be very useful.

Field study can act as complementary to resource management. Understanding the study area in the real world, away from office and images can be an integral part of hypothesis.

More advanced geological information is needed for accurate modeling and monitoring such as better estimates of eroded saprolite volume, exact porosity of the soil and saprolite texture, and clay content in saprolite which has influence in fluid flow migration.

5   Conclusion

In this study, a hypothesis was presented for the potential hydrocarbon reservoir in weathered bedrock structure of about one square kilometer at the center of Bømlo Island. Bømlo Island serves as an onshore site analogous to the vast offshore Johan Sverdrup oil field .The combination of the TWIN report, LIDAR data and GIS, provides a framework to calculate the bedrock connectivity, to estimate the eroded saprolite volume in fractures, and finally to measure the amount of potential fluid reservoir in the saprolite pores. The obtained results from the study presented the potential available hydrocarbon (or groundwater) that underlined the fracture zones and saprolite pockets.

As it was assumed, the connectivity of weathered bedrock in the area was strong and high, as a result the pathways were short and fluid migration thought to occur easily. If the selected area at the height of 60m (A.s.l) is buried by eroded saprolite, with 25% porosity, it could approximately produce 2, 3 million m^3 (608,000,000 gallons) of hydrocarbon or ground water resource.

This study shows the feasibility of bedrock lineament mapping using LiDAR data. The used method in this study could easily be implemented in larger geographical areas, and assume to be useful tool for structural geographical applications.

A variety of approaches is used in this study to assess, explore and manage natural resources and reservoirs. The criteria used in this study aims at utilizing high quality data to make decision and select specific areas of field work for exploration. Based on this, this study, as employed in the field of "natural resource management" can contribute to various fields of interests and needs, such as geography, geology, environment and economics.

LiDAR data and GIS-based applications were selected to work on the study site, one square kilometer bare-earth of Bømlo Island, which derived high resolution DEM. The LiDAR data demonstrated the high value of resolution terrain models such as DSM, DEM and Hillshade. The high quality LiDAR data and the derived high resolution DEM using GIS played an essential role in the geological mapping, such as exposed surface features and detail bedrock structures. Applying GIS as a medium for management tool is very useful for data storage and conversion, image processing, analyses of linear features and surface volume estimation.

6 References

Ahmed, R. J. (2011). "Image enhancement and noise removal by using new spatial filters." <u>UPB Sci. Bull., Series C</u> **73**(1).

Argialas, D. and O. Mavrantza (2004). "Comparison of edge detection and hough transform techniques for the extraction of geologic features." <u>International Archives of the Photogrammetry, Remote Sensing and Spatial Information Sciences</u> **34**.

Bater, C. W. and N. C. Coops (2009). "Evaluating error associated with lidar-derived DEM interpolation." <u>Computers & Geosciences</u> **35**(2): 289-300.

Bear, J. (2013). <u>Dynamics of fluids in porous media</u>, Courier Dover Publications.

Berkowitz, B. (2002). "Characterizing flow and transport in fractured geological media: A review." <u>Advances in water resources</u> **25**(8): 861-884.

Brace, W. (1980). <u>Permeability of crystalline and argillaceous rocks</u>. International Journal of Rock Mechanics and Mining Sciences & Geomechanics Abstracts, Elsevier.

Braga, S., et al. (2002). "Weathering of granites in a temperate climate (NW Portugal): granitic saprolites and arenization." <u>Catena</u> **49**(1): 41-56.

Brock, J. C. and S. J. Purkis (2009). "The emerging role of lidar remote sensing in coastal research and resource management." <u>Journal of Coastal Research</u>: 1-5.

Cavalli, M., et al. (2008). "The effectiveness of airborne LiDAR data in the recognition of channel-bed morphology." <u>Catena</u> **73**(3): 249-260.

Chaabouni, R., et al. (2012). "Lineament analysis of South Jenein Area (Southern Tunisia) using remote sensing data and geographic information system." <u>The Egyptian Journal of Remote Sensing and Space Science</u> **15**(2): 197-206.

Chen, B., et al. (1999). "Edge enhancement of remote sensing image data in the DCT domain." <u>Image and Vision Computing</u> **17**(12): 913-921.

Childs, C. (2005). "ArcGIS Network Analyst: Networks and Network Models."

cmex (2014). "Modern Groundwater/ Porosity Voids." Retrieved 11.10.2014, from http://cmex.ihmc.us/cmex/data/catalog/ModernGroundwater/PorosityVoids.html.

Comber, A., et al. (2008). "Using a GIS-based network analysis to determine urban greenspace accessibility for different ethnic and religious groups." Landscape and Urban Planning **86**(1): 103-114.

Dar, I. A., et al. (2010). "Remote sensing technology and geographic information system modeling: an integrated approach towards the mapping of groundwater potential zones in Hardrock terrain, Mamundiyar basin." Journal of hydrology **394**(3): 285-295.

DeMers, M. N. (2008). Fundamentals of geographic information systems, John Wiley & Sons.

DeMers, M. N. (2009). GIS for Dummies, John Wiley & Sons.

Djokic, D. and D. R. Maidment (1993). "Application of GIS network routines for water flow and transport." Journal of Water Resources Planning and Management **119**(2): 229-245.

EIJ (2014). "Earth Imaging Journal,Global Elevation Data Enhance Exploration and Development." Retrieved 15092014, 2014, from http://eijournal.com/print/articles/global-elevation-data-enhance-exploration-and-development.

ESRI (2011). "Exploring digital elevation models." Retrieved 12.08, 2014, from http://help.arcgis.com/en/arcgisdesktop/10.0/help/index.html#//009z0000005n000000.htm.

ESRI (2012). "How Surface Volume works." Retrieved 01102014, 2014, from http://resources.arcgis.com/en/help/main/10.1/index.html#//00q900000037000000.

ESRI (2012). "What is Network Analyst?". 2013, from http://help.arcgis.com/en/arcgisdesktop/10.0/help/index.html#//004700000001000000.

ESRI (2013). "ArcGIS Resources." Retrieved 01.10.2014, 2014, from http://resources.arcgis.com/en/help/main/10.1/index.html#//009z000000v0000000.

ESRI (2013). ArcGIS Resources. **10.1**.

ESRI (2013). "ArcGIS Resources/ArcGIS Help 10.1/3D Analyst and ArcScene." Retrieved 01.10.2014, 2014, from
http://resources.arcgis.com/en/help/main/10.1/index.html#//00q8000000p0000000.

ESRI (2013). "Feature To Line (Data Management)." Retrieved 01102014, 2014, from
http://resources.arcgis.com/en/help/main/10.1/index.html#//001700000039000000.

ESRI (2013). "LiDAR data." Retrieved 01102014, 2014, from
http://resources.arcgis.com/en/help/main/10.1/index.html#//015w00000041000000.

ESRI (2014). "GIS Dictionary/Altitude." Retrieved 01.10.2014, 2014, from
http://support.esri.com/en/knowledgebase/GISDictionary/search.

ESRI (2014). "GIS Dictionary/Azimuth." Retrieved 01.10.2014, 2014, from
http://support.esri.com/en/knowledgebase/GISDictionary/term/azimuth.

ESRI (2014). "Support/GIS Dictionary/Digitizing." Retrieved 01.10.2014, 2014, from
http://support.esri.com/en/knowledgebase/GISDictionary/term/digitizing.

ESRI (2014). "Support/GIS Dictionary/Network analysis class." Retrieved 01.10.2014, 2014, from
http://support.esri.com/en/knowledgebase/GISDictionary/term/network%20analysis%20class.

forskning.no (2011). "Forvitret fjell både farlig og rikt." 2014, from
http://forskning.no/geofag/2011/08/forvitret-fjell-bade-farlig-og-rikt.

Geographic, N. (2014). "education,bedrock." Retrieved 01102014, 2014, from
http://education.nationalgeographic.com/education/encyclopedia/bedrock/?ar_a=1.

Geomorphology, G. (2013). "Linear Features Interp." Retrieved 01.10.2013, 2014, from
http://gis4geomorphology.com/linear-features-interp/.

geoportalen (2011). "Forvitret grunnfjell." 2013, from
http://www.geoportalen.no/forskning/forvitring/.

Glenn, N. F., et al. (2006). "Analysis of LiDAR-derived topographic information for characterizing and differentiating landslide morphology and activity." Geomorphology **73**(1): 131-148.

Gluyas, J. and R. Swarbrick (2009). Petroleum geoscience, John Wiley & Sons.

Gonzalez, R. C., et al. (2004). "Digital image processing using MATLAB." Upper Saddle River, N. J: Pearson Prentice Hall.

Graham, R. C., et al. (2010). "Rock to regolith conversion: Producing hospitable substrates for terrestrial ecosystems." GSA Today **20**(2): 4-9.

Gudmundsson, A. (2011). Rock fractures in geological processes, Cambridge University Press.

Gudmundsson, A. (2011). Rock fractures in geological processes, Cambridge University Press Cambridge.

Gunterberg, L. (2013). "Oil occurrences in crystalline basement rocks, southern Norway– comparison with deeply weathered basement rocks in southern Sweden.(15 hp)."

Hall, C., et al. (2003). "Hydrocarbons and the evolution of human culture." Nature **426**(6964): 318-322.

Haugen, Å. (2010). "Fluid flow in fractured carbonates: wettability effects and enhanced oil recovery."

Hesthammer, J. and M. Boulaenko (2005). "The offshore EM challenge." First break **23**(11).

Hodgson, M. E., et al. (2003). "An evaluation of LIDAR-and IFSAR-derived digital elevation models in leaf-on conditions with USGS Level 1 and Level 2 DEMs." Remote Sensing of Environment **84**(2): 295-308.

Hudak, A. T., et al. (2009). "LiDAR utility for natural resource managers." Remote Sensing **1**(4): 934-951.

Jain, M. K. and V. P. Singh (2005). "DEM-based modelling of surface runoff using diffusion wave equation." Journal of hydrology **302**(1): 107-126.

Jiang, B. and C. Claramunt (2004). "Topological analysis of urban street networks." Environment and Planning B **31**(1): 151-162.

Kansky, K. (1963). "Structure of transportation networks: relationships between network geometry and regional characteristics." University of Chicago, Department of Geography, Research Paper 84.

Kennedy, R. E., et al. (2009). "Remote sensing change detection tools for natural resource managers: Understanding concepts and tradeoffs in the design of landscape monitoring projects." Remote Sensing of Environment 113(7): 1382-1396.

Kessarkar, P. and K. S. Srinivas "K., and Chaubey, AK, 2011. Proposed landslide mapping method for Canacona region." National Institute of Oceanography,(Council of Scientific & Industrial Research, Dona Paula, Goa: 5.

Koch, A. and C. Heipke (2006). "Semantically correct 2.5 D GIS data—the integration of a DTM and topographic vector data." ISPRS Journal of Photogrammetry and Remote Sensing 61(1): 23-32.

Koning, T. (2003). "Oil and gas production from basement reservoirs: examples from Indonesia, USA and Venezuela." Geological Society, London, Special Publications 214(1): 83-92.

Korte, G. (2001). The GIS book, Cengage Learning.

Kreylos, O., et al. (2008). Immersive visualization and analysis of LiDAR data. Advances in visual computing, Springer: 846-855.

Lane, C. R. and E. D'Amico (2010). "Calculating the ecosystem service of water storage in isolated wetlands using LiDAR in North Central Florida, USA." Wetlands 30(5): 967-977.

Lang, L. (1998). "Managing natural resources with GIS."

Li, Z., et al. (2010). Digital terrain modeling: principles and methodology, CRC press.

Lidmar-Bergström, K., et al. (2007). "Cenozoic landscape development on the passsive margin of northern Scandinavia." Norwegian Journal of Geology 87(1 & 2): 181-196.

Lidmar-Bergström, K., et al. (2000). "Landforms and uplift history of southern Norway." Global and Planetary Change 24(3): 211-231.

Lidmar-Bergström, K., et al. (1999). "Relief features and palaeoweathering remnants in formerly glaciated Scandinavian basement areas." Palaeoweathering, palaeosurfaces and related continental deposits: 275-301.

Lillesand, T. M., et al. (2004). Remote sensing and image interpretation, John Wiley & Sons Ltd.

Liu, X., et al. (2005). High-resolution DEM generated from LiDAR data for water resource management. Proceedings of the International Congress on Modelling and Simulation (MODSIM05), Modelling and Simulation Society of Australia and New Zealand Inc.

Liu, X. and Z. Zhang (2008). "LIDAR data reduction for efficient and high quality DEM generation." International Archives of the Photogrammetry, Remote Sensing and Spatial Information Sciences **37**: 173-178.

Longley, P. (2005). Geographic information systems and science, John Wiley & Sons.

Longley, P. (2011). Geographic information systems & science. Hoboken, NJ, Wiley.

Loosveld, R. and R. Franssen (1992). Extensional vs. shear fractures: implications for reservoir characterisation. European Petroleum Conference, Society of Petroleum Engineers.

Lukas, K. and R. Weibel (1995). Assessment and improvement of methods for analytical hillshading. Proceedings, International Cartographic Conference. Barcelona.

Mallawaarachchi, T., et al. (1996). "GIS-based integrated modelling systems for natural resource management." Agricultural Systems **50**(2): 169-189.

metropolis (2013). "soil profile." Retrieved 01102014, 2014, from http://www.metropolismag.com/.

MichaelAllaby, C. saprolite, 'Oxford University Press'.

Migoń, P. and K. Lidmar-Bergström (2001). "Weathering mantles and their significance for geomorphological evolution of central and northern Europe since the Mesozoic." Earth-Science Reviews **56**(1): 285-324.

Migoń, P. and K. Lidmar-Bergström (2002). "Deep weathering through time in central and northwestern Europe: problems of dating and interpretation of geological record." Catena **49**(1): 25-40.

Miller, C. L. and R. A. Laflamme (1958). The Digital Terrain Model-: Theory & Application, MIT Photogrammetry Laboratory.

Mohn, K. and P. Osmundsen (2008). "Exploration economics in a regulated petroleum province: the case of the Norwegian Continental Shelf." Energy Economics **30**(2): 303-320.

Nelson, R. (2001). Geologic analysis of naturally fractured reservoirs, Gulf Professional Publishing.

Neri, M., et al. (2008). "The changing face of Mount Etna's summit area documented with Lidar technology." Geophysical research letters **35**(9).

Nyborg, M., et al. (2007). "Detection of lineaments using airborne laser scanning technology: Laxemar-Simpevarp, Sweden." Hydrogeology journal **15**(1): 29-32.

O'Callaghan, J. F. and D. M. Mark (1984). "The extraction of drainage networks from digital elevation data." Computer vision, graphics, and image processing **28**(3): 323-344.

Odling, N. (1994). "Natural fracture profiles, fractal dimension and joint roughness coefficients." Rock mechanics and rock engineering **27**(3): 135-153.

Odling, N. E. (1992). "Network properties of a two-dimensional natural fracture pattern." Pure and Applied Geophysics **138**(1): 95-114.

Olesen, O., et al. (2012). "Tropical Weathering in Norway, TWIN final report." NGU Report **2012**: 1-188.

Ollier, C. D. (1988). "Deep weathering, groundwater and climate." Geografiska Annaler. Series A. Physical Geography: 285-290.

Onorati, G., et al. (1992). "The digital elevation model of Italy for geomorphology and structural geology." Catena **19**(2): 147-178.

Pavlis, T. L. and R. L. Bruhn (2011). "Application of LIDAR to resolving bedrock structure in areas of poor exposure: An example from the STEEP study area, southern Alaska." <u>Geological Society of America Bulletin</u> **123**(1-2): 206-217.

Petford, N. and K. McCaffrey (2003). "Hydrocarbons in crystalline rocks: an introduction." <u>Geological Society, London, Special Publications</u> **214**(1): 1-5.

Peuquet, D. J. and D. F. Marble (2003). <u>Introductory readings in geographic information systems</u>, CRC Press.

Poehls, D. J. and G. J. Smith Saprolite. <u>Encyclopedic Dictionary of Hydrogeology</u>, Elsevier.

Ramachandran, S. (1998). "Application of remote sensing and GIS." <u>Madras University</u>.

Ramberg, I. B. (2008). <u>The making of a land: geology of Norway</u>, Geological Society of London.

Rao, N. S., et al. (2001). "Identification of groundwater potential zones using remote sensing techniques in and around Guntur town, Andhra Pradesh, India." <u>Journal of the Indian Society of Remote Sensing</u> **29**(1-2): 69-78.

Riis, F. (1996). "Quantification of Cenozoic vertical movements of Scandinavia by correlation of morphological surfaces with offshore data." <u>Global and Planetary Change</u> **12**(1): 331-357.

Roy, A., et al. (2010). "Lacunarity analysis of fracture networks: Evidence for scale-dependent clustering." <u>Journal of Structural Geology</u> **32**(10): 1444-1449.

Rutter, E. (2012). "Rock fractures in geological processes Gudmunsson, A., Cambridge University Press, 2011, ISBN 978-0-521-86392-6, Hardcover, 578 pp.,£ 45.00." <u>Geophysical Journal International</u> **188**(1): 382-382.

Schmid, K., et al. (2008). "Lidar 101: An introduction to lidar technology, data, and applications." <u>National Oceanic and Atmospheric Administration (NOAA) Coastal Services Center</u>.

Schoorl, J., et al. (2000). "Three-dimensional landscape process modelling: the effect of DEM resolution." <u>Earth Surface Processes and Landforms</u> **25**(9): 1025-1034.

Schröder, F. and P. Rossbach (1994). "Managing the complexity of digital terrain models." Computers & Graphics **18**(6): 775-783.

Sener, E., et al. (2005). "An integration of GIS and remote sensing in groundwater investigations: a case study in Burdur, Turkey." Hydrogeology journal **13**(5-6): 826-834.

Shan, J. and C. K. Toth (2008). Topographic laser ranging and scanning: principles and processing, CRC Press.

Sharp, J. M. (2014). Fractured Rock Hydrogeology, CRC Press.

Smith, M. J. and S. M. Wise (2007). "Problems of bias in mapping linear landforms from satellite imagery." International Journal of Applied Earth Observation and Geoinformation **9**(1): 65-78.

Snow, D. T. (1969). "Anisotropie permeability of fractured media." Water Resources Research **5**(6): 1273-1289.

Song, J.-H., et al. (2002). "Assessing the possibility of land-cover classification using lidar intensity data." International Archives of Photogrammetry Remote Sensing and Spatial Information Sciences **34**(3/B): 259-262.

Spaete, L. P., et al. (2011). "Vegetation and slope effects on accuracy of a LiDAR-derived DEM in the sagebrush steppe." Remote Sensing Letters **2**(4): 317-326.

Sturtevant, J. T. (2014). "LiDAR as a Tool for Lineament Mapping and the Reevaluation of Bedrock and Glacial Geology: Examples from the Mount Moosilauke Region of the White Mountain National Forest, New Hampshire."

Survey, U. S. G. (2013). "Bedrock." 2014, from http://www.eoearth.org/view/article/164937/.

Taylor, G. and R. A. Eggleton (2001). Regolith geology and geomorphology, John Wiley & Sons.

Thompson, J. A., et al. (2001). "Digital elevation model resolution: effects on terrain attribute calculation and quantitative soil-landscape modeling." Geoderma **100**(1): 67-89.

Tinkham, W. T., et al. (2011). "A comparison of two open source LiDAR surface classification algorithms." Remote Sensing **3**(3): 638-649.

USGS (2007). "What is a GIS?". Retrieved 12.08.2014, 2014, from http://webgis.wr.usgs.gov/globalgis/tutorials/what_is_gis.htm

USGS (2014). "Water Questions & Answers, How much water does the average person use at home per day?". Retrieved 10.10.2014, from http://water.usgs.gov/edu/qa-home-percapita.html.

Van Den Eeckhaut, M., et al. (2005). "The effectiveness of hillshade maps and expert knowledge in mapping old deep-seated landslides." Geomorphology **67**(3): 351-363.

Ventura, G. and G. Vilardo (2008). "Emplacement mechanism of gravity flows inferred from high resolution Lidar data: The 1944 Somma–Vesuvius lava flow (Italy)." Geomorphology **95**(3): 223-235.

Vincent, R. K. (1997). Fundamentals of geological and environmental remote sensing, Prentice Hall Upper Saddle River, NJ.

Walford, N. (2002). Geographical data: characteristics and sources, John Wiley & Sons.

Weibel, R. and M. Heller (1993). Digital terrain modelling, Oxford University Press.

White, S. A. and Y. Wang (2003). "Utilizing DEMs derived from LIDAR data to analyze morphologic change in the North Carolina coastline." Remote Sensing of Environment **85**(1): 39-47.

Willis, B. J. and C. D. White (2000). "Quantitative outcrop data for flow simulation." Journal of Sedimentary Research **70**(4).

Witzke, B. J., et al. (2010). "Iowa Bedrock Topography Hillshade."

Yeung, A. K. and C. Lo (2002). Concepts and techniques of geographic information systems, Prentice Hall.

Zelazny, M. M. (2011). Lineament Mapping using Remote Sensing Techniques and Structural Geology for CO2 Sequestration Site Characterization in Central New York State, State University of New York at Buffalo.

Zhiqing, L., et al. (2006). "The Airborne LiDAR Technology." <u>Land and Resources Informatization</u> **2**: 005.

Zhou, Q. and Y. Chen (2011). "Generalization of DEM for terrain analysis using a compound method." <u>ISPRS Journal of Photogrammetry and Remote Sensing</u> **66**(1): 38-45.